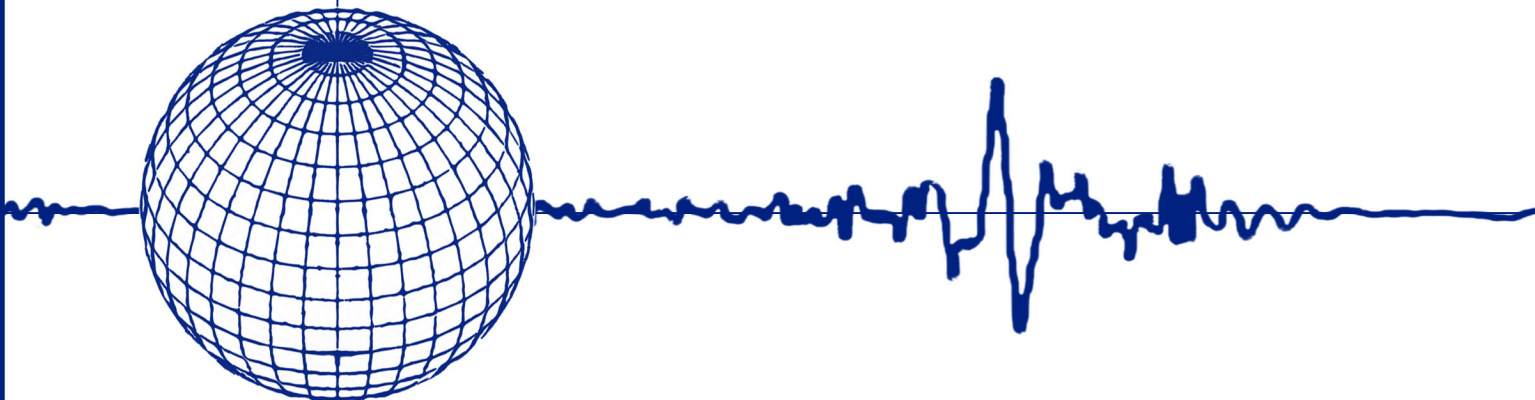EARTHQUAKE ENGINEERING RESEARCH CENTER

A MODAL PUSHOVER ANALYSIS PROCEDURE TO ESTIMATE SEISMIC DEMANDS FOR UNSYMMETRIC-PLAN BUILDINGS:
Theory and Preliminary Evaluation

By

Anil K. Chopra
Rakesh K. Goel

COLLEGE OF ENGINEERING

UNIVERSITY OF CALIFORNIA, BERKELEY

A MODAL PUSHOVER ANALYSIS PROCEDURE TO ESTIMATE SEISMIC DEMANDS FOR UNSYMMETRIC-PLAN BUILDINGS:
Theory and Preliminary Evaluation

by

Anil K. Chopra
University of California, Berkeley

and

Rakesh K. Goel
California Polytechnic State University
San Luis Obispo

Earthquake Engineering Research Center
University of California
September 2003

UCB/EERC 2003-08

ABSTRACT

Based on structural dynamics theory, the modal pushover analysis procedure (MPA) retains the conceptual simplicity of current procedures with invariant force distribution, now common in structural engineering practice. The MPA procedure for estimating seismic demands is extended to unsymmetric-plan buildings. In the MPA procedure, the seismic demand due to individual terms in the modal expansion of the effective earthquake forces is determined by nonlinear static analysis using the inertia force distribution for each mode, which for unsymmetric buildings includes two lateral forces and torque at each floor level. These "modal" demands due to the first few terms of the modal expansion are then combined by the CQC rule to obtain an estimate of the total seismic demand for inelastic systems. When applied to elastic systems, the MPA procedure is equivalent to standard response spectrum analysis (RSA). The MPA estimates of seismic demand for torsionally-stiff and torsionally-flexible unsymmetric systems are shown to be similarly accurate as they are for the symmetric building; however, the results deteriorate for a torsionally-similarly-stiff unsymmetric-plan system and the ground motion considered because (a) elastic modes are strongly coupled, and (b) roof displacement is underestimated by the CQC modal combination rule (which would also limit accuracy of RSA for linearly elastic systems).

ACKNOWLEDGMENTS

CONTENTS

1.   INTRODUCTION

The nonlinear static procedure (NSP) or pushover analysis, as described in FEMA-273 [1] and its successor FEMA-356 [2] is now used by the structural engineering profession as a standard tool for estimating seismic demands for buildings. In the past few years, several researchers have discussed the underlying assumptions and limitations of pushover analysis [e.g., Refs. 3-8], proposed adaptive force distributions that attempt to follow the time-variant distributions of inertia forces [9, 10], and considered more than the fundamental vibration mode [11-13]. Rooted in structural dynamics theory, the modal pushover analysis (MPA) has been developed to include the contributions of all modes of vibration that contribute significantly to seismic demands [14]. It retains the conceptual simplicity and computational attractiveness of the standard pushover procedures with time-invariant lateral force distributions. This procedure has been improved, especially in its treatment of P-Δ effects due to gravity loads [15] and its accuracy—bias and dispersion—has been evaluated for SAC buildings [15], height-wise regular generic frames [16] and irregular generic frames [17].

Starting in 1997, various researchers have extended pushover analysis to unsymmetric-plan buildings. By applying a height-wise distribution of lateral forces, typical of standard planar pushover analysis at the floor centers of mass, an approximate nonlinear static analysis procedure was developed [18]; by the authors' admission the procedure "does not pretend to be very accurate." Another procedure consists of (i) three-dimensional elastic response spectrum analysis to determine roof displacement and height-wise distribution of lateral forces for each resisting element (frames, walls, etc.), and (ii) planar pushover analysis of each resisting element [19]. Some studies have focused on special considerations necessary to consider interaction between walls and frames in pushover analysis of wall-frame structures [20]. Another paper investigated the accuracy of applying lateral forces at different locations in the plan of unsymmetric buildings [21]. The few comparisons of pushover analysis results with nonlinear RHA give the impression of limited success. The need for developing improved rational approximate procedures for unsymmetric-plan buildings is critical. Current engineering practice [2] is based on judgmental extensions of methods initially developed for planar analysis of buildings, which appear inaccurate.

The principal objective of this paper is to extend MPA to estimate seismic demands for unsymmetric-plan buildings. To provide a basis for the MPA procedure, we first develop an uncoupled modal response history analysis (UMRHA) procedure, which is shown to be equivalent to classical modal response history analysis (RHA) for linearly elastic systems, but only an approximate procedure for inelastic systems; the underlying assumptions and accuracy are discussed. Subsequently, we present the MPA procedure for unsymmetric-plan buildings, demonstrate its equivalence to standard response spectrum analysis (RSA) for elastic systems, and identify its underlying assumptions and approximations for inelastic buildings. Finally, the accuracy of MPA relative to rigorous nonlinear RHA is evaluated.

2.   EQUATIONS OF MOTION, SELECTED BUILDINGS, AND GROUND MOTION

Consider an assemblage of moment-resisting frames that make up an *N*-story building (Fig. 1). Its plan shown in Fig. 1a is not symmetric about the *x* or/and *y* axes. This implies that the floor mass distribution and/or framing plan may be unsymmetric; or the framing plan is symmetric but the stiffness properties of symmetrically-located frames differ. Each floor diaphragm is rigid in its own plane and has three degrees-of-freedom (DOFs) defined at the center of mass (CM); see Fig. 1a. The DOFs of the *j*th floor are: translation u_{jx} along the *x*-axis, translation u_{jy} along the *y*-axis, and torsional rotation $u_{j\theta}$ about the vertical axis; u_{jx} and u_{jy} are defined relative to the ground.

2.1   Equations of Motion

The displacement vector **u** of size $3N \times 1$ for the system includes three $N \times 1$ subvectors $\mathbf{u}_x, \mathbf{u}_y$, and $\mathbf{u}_\theta$ where $\mathbf{u}_x$ is the vector of *x*-lateral floor displacement u_{jx}; $\mathbf{u}_y$ is the vector of *y*-lateral floor displacements u_{jy}; and $\mathbf{u}_\theta$ is the vector of *N*-torsional floor displacements:

$$\mathbf{u}_x = \left\langle u_{1x} \ u_{2x} \cdots u_{Nx} \right\rangle^T \quad \mathbf{u}_y = \left\langle u_{1y} \ u_{2y} \cdots u_{Ny} \right\rangle^T \quad \mathbf{u}_\theta = \left\langle u_{1\theta} \ u_{2\theta} \cdots u_{N\theta} \right\rangle^T$$

The differential equations of motion governing the response of the building to the *x* and *y* components of ground motion are:
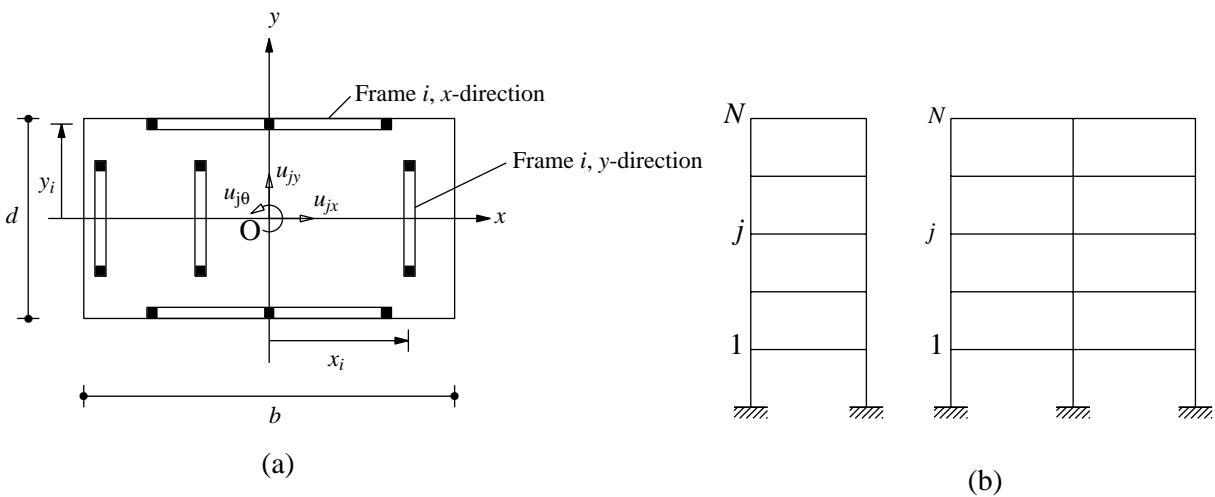

Figure 1.   Multistory building: (a) plan; (b) frames in *x* and *y* directions.

3

$$\mathbf{M}\ddot{\mathbf{u}} + \mathbf{f}_s\left(\mathbf{u}, sign\,\dot{\mathbf{u}}\right) = -\mathbf{M}\,\boldsymbol{\iota}_x \ddot{u}_{gx}\left(t\right) - \mathbf{M}\,\boldsymbol{\iota}_y \ddot{u}_{gy}\left(t\right) \tag{1}$$

where $\mathbf{M}$, a diagonal mass matrix of order 3N, includes three diagonal submatrices $\mathbf{m}$, $\mathbf{m}$ and $\mathbf{I}_O$, each of order N; $\mathbf{m}$ is a diagonal matrix with $m_{jj} = m_j$, the mass lumped at the jth-floor diaphragm; and $\mathbf{I}_O$ is a diagonal matrix with $I_{jj} = I_{Oj}$, the polar moment of inertia of the jth-floor diaphragm about a vertical axis through the CM. The force-deformation relations between the displacements $\mathbf{u}_x$, $\mathbf{u}_y$, and $\mathbf{u}_\theta$ and the x-lateral forces $\mathbf{f}_{sx}$, y-lateral forces $\mathbf{f}_{sy}$, and torques $\mathbf{f}_{s\theta}$ at the N floor levels are nonlinear and hysteretic. In Eq. (1), the influence vectors associated with the x and y ground motions are as follows:

$$\boldsymbol{\iota}_x = \begin{Bmatrix} \mathbf{1} \\ \mathbf{0} \\ \mathbf{0} \end{Bmatrix} \qquad \boldsymbol{\iota}_y = \begin{Bmatrix} \mathbf{0} \\ \mathbf{1} \\ \mathbf{0} \end{Bmatrix} \tag{2}$$

respectively, where each element of the $N \times 1$ vector $\mathbf{1}$ is equal to unity and of the $N \times 1$ vector $\mathbf{0}$ is equal to zero. Although not shown in Eq. (1), damping is included and defined by modal damping ratios.

The right side of Eq. (1) can be interpreted as effective earthquake forces

$$\mathbf{p}_{\text{eff}}\left(t\right) = -\mathbf{s}\,\ddot{u}_g\left(t\right) = -\begin{Bmatrix} \mathbf{m1} \\ \mathbf{0} \\ \mathbf{0} \end{Bmatrix} \ddot{u}_{gx}\left(t\right) \text{ and } -\begin{Bmatrix} \mathbf{0} \\ \mathbf{m1} \\ \mathbf{0} \end{Bmatrix} \ddot{u}_{gy}\left(t\right) \tag{3}$$

associated with the x and y components of ground motion, respectively.

2.2 Selected Structural Systems

The structural systems considered in this paper are variations of the 9-story steel frame building designed for the SAC Steel Project. Although not actually constructed, this structure meets seismic code and represents typical medium-rise buildings for Los Angeles, California. This building is described in several publications [e.g., Refs. 14 and 22]. Described in Appendix A for convenience, it is one of six symmetric-plan buildings used as examples to determine the bias and dispersion in the MPA procedure [15].
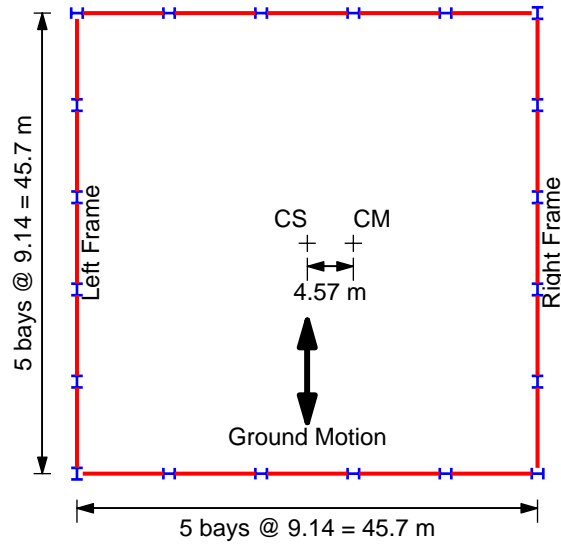
Figure 2.   Plan of selected unsymmetric-plan buildings.

This symmetric-plan building was modified to create three systems that are unsymmetric about the *y*-axis but symmetric about *x*-axis. While the stiffness properties were preserved, the center of mass (CM) was defined eccentric relative to the center of stiffness (CS), also the geometric center. The eccentricity between the CM and CS was chosen to be along the *x*-axis, equal to 10% of the plan dimension (Fig. 2). The ratio between the floor mass, m_j, and its moment of inertia, I_{Oj} (about a vertical axis through CM), was varied to create three different unsymmetric-plan systems with different degrees of coupling between lateral and torsional motions as characterized by different values of the ratio of uncoupled lateral and torsional vibration periods.

1. Unsymmetric-Plan 1 (U1): The I_{Oj}/m ratio at the CS was taken to be the same as for the symmetric-plan building. Figure 3a shows the natural vibration periods and modes of system U1. Lateral displacements dominate motion in the first mode, whereas torsional rotations dominate motion in the second mode, indicating weak coupling between lateral and torsional motions. Because the period of the dominantly-torsional mode is much shorter than that of the dominantly-lateral mode, which is representative of buildings with moment-resisting frames located along the perimeter of the plan, this system will be referred to as a "torsionally-stiff" system.

5

2. Unsymmetric-Plan 2 (U2): The I_{Oj} value for every floor was increased by a factor of 2.95 relative to Case U1 and was chosen to achieve very close modal periods. Figure 3b demonstrates that the periods of the first two modes are indeed close and that the lateral and torsional motions, which are similar in magnitude, are strongly coupled in the first two modes. This system with similar periods in these two modes will be referred to as a "torsionally-similarly-stiff" system.

3. Unsymmetric-Plan 3 (U3): The I_{Oj} value for every floor was increased by a factor of 6.0 relative to case U1. Figure 3c shows the natural vibration periods and modes of system U3. Torsional rotations dominate motion in the first mode, whereas lateral displacements dominate motion in the second mode, indicating weak coupling between lateral and torsional motions. Because the period of the dominantly-torsional mode is much longer than that of the dominantly-lateral mode, this system is said to be "torsionally-flexible."

These three unsymmetric-plan systems will undergo coupled *y*-lateral and torsional motions due to the *y*-component of ground motion, which is the focus of this paper. The purely lateral response along the *x*-axis due to the *x*-component of excitation is not considered, as it has been the subject of previous investigations [10, 11].

2.3 Ground Motion

The ground motion selected for this investigation is the LA25 ground motion shown in Fig. 4. This is one of the 20 ground motions that were assembled for the SAC project representing exceedance probability of 2% in 50 years, or a return period of 2475 years. It is derived from the free-field motion recorded at Rinaldi Receiving Station during the 1994 Northridge earthquake. Recorded at a distance of 7.5 km from the causative fault, it contains a forward directivity pulse (Fig. 4), which is common in many near-fault motions. This intense ground motion enables testing of the approximate procedures developed herein under severe conditions.

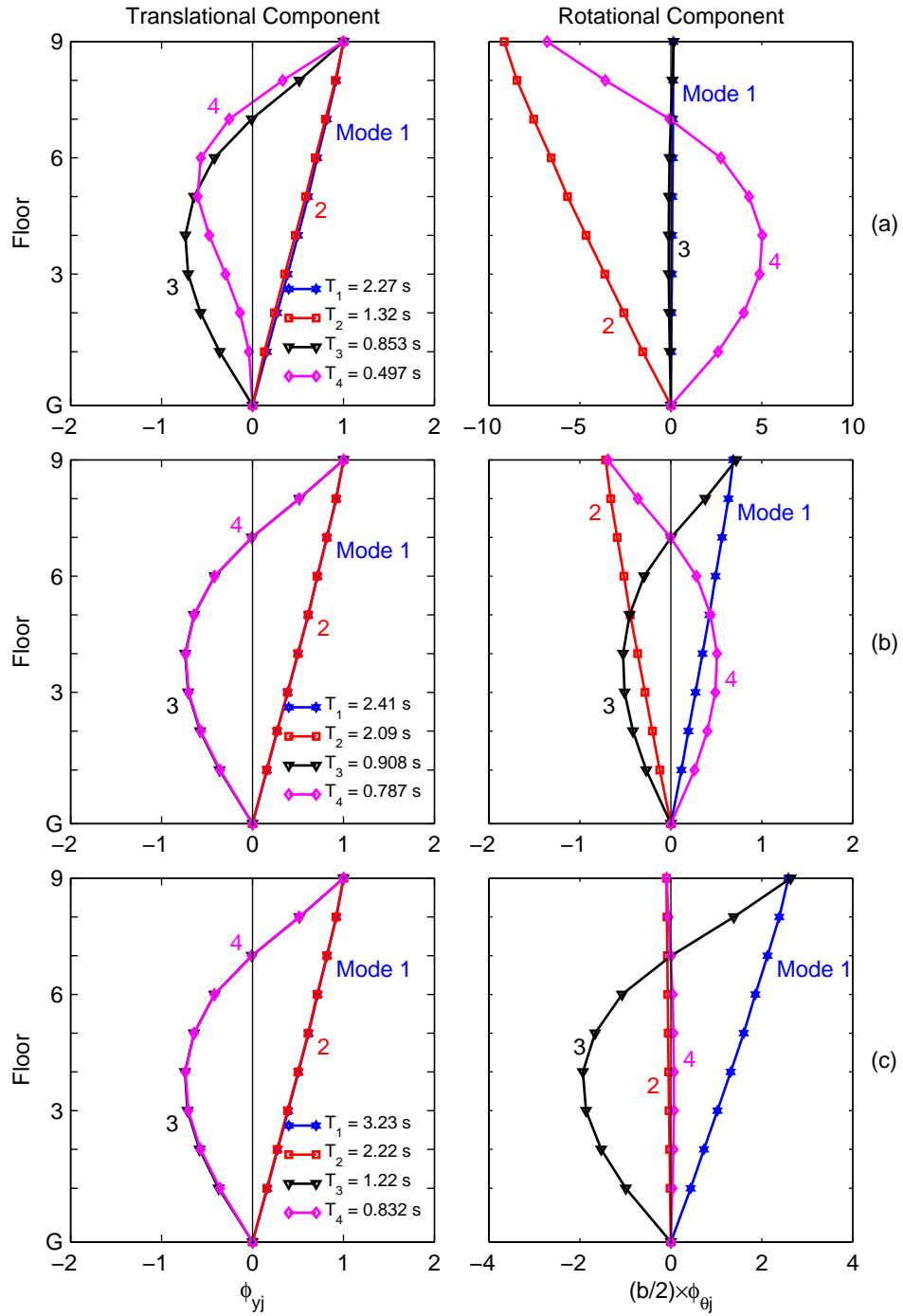**Figure 3.** Natural periods and modes of vibration of 9-story unsymmetric-plan systems: (a) unsymmetric-plan system U1; (b) unsymmetric-plan system U2; and (c) unsymmetric-plan system U3.
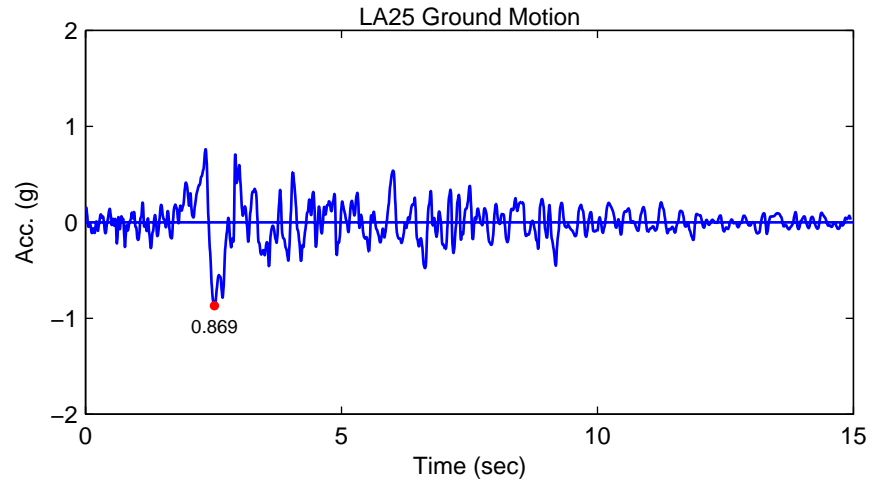
Figure 4. LA25 ground motion, one of twenty ground motions assembled for the SAC project. It is derived from the free-field motion recorded at Rinaldi Receiving Station during the 1994 Northridge, California, earthquake.

3. APPROXIMATE ANALYSIS PROCEDURES

3.1 Modal Expansion of Effective Forces

The spatial distribution of the effective forces [Eq. (3)] over the building is defined by the vector $\mathbf{s}$ and the time variation by $\ddot{u}_g(t) = \ddot{u}_{gx}(t)$ or $\ddot{u}_{gy}(t)$. This force distribution can be expanded as a summation of modal inertia force distributions $\mathbf{s}_n$ [Ref. 23, Section 13.3]

$$\mathbf{s} = \sum_{n=1}^{3N} \mathbf{s}_n = \sum_{n=1}^{3N} \Gamma_n \mathbf{M} \boldsymbol{\phi}_n \tag{4}$$

where $\boldsymbol{\phi}_n$ is the nth natural vibration mode of the structure consisting of three subvectors, $\boldsymbol{\phi}_{xn}, \boldsymbol{\phi}_{yn}$, and $\boldsymbol{\phi}_{\theta n}$, and

$$\Gamma_n = \frac{L_n}{M_n} \qquad M_n = \boldsymbol{\phi}_n^T \mathbf{M} \boldsymbol{\phi}_n \qquad L_n = \begin{cases} \boldsymbol{\phi}_{xn}^T \mathbf{m1} & \text{for} \quad \ddot{u}_{gx}(t) \\ \boldsymbol{\phi}_{yn}^T \mathbf{m1} & \text{for} \quad \ddot{u}_{gy}(t) \end{cases} \tag{5}$$

The effective earthquake forces can then be expressed as

$$\mathbf{p}_{\text{eff}}(t) = \sum_{n=1}^{3N} \mathbf{p}_{\text{eff,n}}(t) = \sum_{n=1}^{3N} -\mathbf{s}_n \ddot{u}_g(t) \tag{6}$$

The contribution of the nth mode to $\mathbf{p}_{\text{eff}}(t)$ and $\mathbf{s}$ are

$$\mathbf{p}_{\text{eff,n}}(t) = -\mathbf{s}_n \ddot{u}_g(t) \qquad \mathbf{s}_n = \Gamma_n \mathbf{M} \boldsymbol{\phi}_n \tag{7}$$

The $\mathbf{s}_n$ vectors associated with the x and y components of ground motions are given by the same equation:

$$\mathbf{s}_n = \begin{Bmatrix} \mathbf{s}_{xn} \\ \mathbf{s}_{yn} \\ \mathbf{s}_{\theta n} \end{Bmatrix} = \Gamma_n \begin{Bmatrix} \mathbf{m} \boldsymbol{\phi}_{xn} \\ \mathbf{m} \boldsymbol{\phi}_{yn} \\ \mathbf{I}_p \boldsymbol{\phi}_{\theta n} \end{Bmatrix} \tag{8}$$

However, Γ_n depends on the component of ground motion, as is evident from Eq. (5).

Figure 5 shows the modal expansion of $\mathbf{s} = \mathbf{m}\boldsymbol{\iota}_y$ for system U2 associated with the y-component of ground motion. These modal contributions $\mathbf{s}_n$ define the force distributions that will be used in pushover analyses to be presented later. Observe that the contribution $\mathbf{s}_n$ of each mode to $\mathbf{s}$ includes lateral forces and torque at each floor level, and that the direction of forces is controlled by the algebraic sign of the modal displacements ϕ_{jxn} and $\phi_{j\theta n}$ (where j denotes floor level). Hence, for the first pair of modes, the lateral forces and torques all act in the same direction; however, for the second and higher modal pairs, the lateral forces and torques change direction as one moves up the structure. The lateral forces are in the positive y-direction in the first pair of modes, whereas the torques are in the positive θ- (counter clockwise) direction in the first mode, but in the clockwise direction in the second mode. The contribution of the first modal pair to the force distribution $\mathbf{s} = \mathbf{m}\boldsymbol{\iota}_y$ of the effective earthquake forces is largest, and these modal contributions decrease progressively for higher modal pairs.
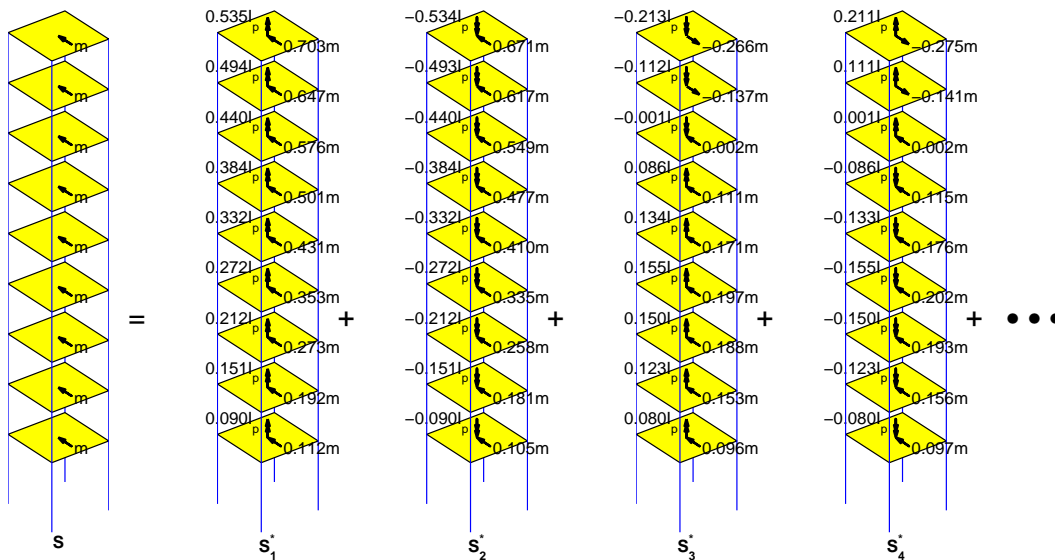

Figure 5.   Modal expansion of $\mathbf{s} = \mathbf{m}\boldsymbol{\iota}_y$ for unsymmetric-plan system U2 subjected to y-component of ground motion.

3.2 Basic Concept

Two procedures for approximate analysis of inelastic buildings will be described next: uncoupled modal response history analysis (UMRHA) and modal pushover analysis (MPA). Not intended for practical application, the UMRHA procedure is developed only to provide a rationale and motivation for the MPA procedure. In the UMRHA procedure, the response history of the building to $\mathbf{p}_{\mathrm{eff,n}}(t)$, the nth-mode component of the excitation is determined by nonlinear RHA of an inelastic SDF system, and superposition of these "modal" responses gives the total response. In the MPA procedure, the peak response to $\mathbf{p}_{\mathrm{eff,n}}(t)$ is determined by a nonlinear static or pushover analysis, and the peak "modal" responses are combined by modal combination rules to estimate the total response.

4. UNCOUPLED MODAL RESPONSE HISTORY ANALYSIS

4.1 Elastic Systems

The classical modal analysis procedure for elastic systems may be interpreted as finding the response of the structure to $\mathbf{p}_{\mathrm{eff},n}(t)$ for each n and superposing the responses for all n. The response of the system to $\mathbf{p}_{\mathrm{eff},n}(t)$ is entirely in the nth mode, with no contribution from other modes, which implies that the modes are uncoupled. Then the floor displacements are given by

$$\mathbf{u}_n(t) = \boldsymbol{\phi}_n q_n(t) \tag{9}$$

where the modal coordinate is governed by

$$\ddot{q}_n + 2\zeta_n \omega_n \dot{q}_n + \omega_n^2 q_n = -\Gamma_n \ddot{u}_g(t) \tag{10}$$

in which ω_n is the natural frequency and ζ_n is the damping ratio for the nth mode. The solution $q_n(t)$ of Eq. (10) is given by

$$q_n(t) = \Gamma_n D_n(t) \tag{11}$$

where $D_n(t)$ is the deformation response of the nth-mode linear SDF system, an SDF system with vibration properties—natural frequency ω_n (natural period $T_n = 2\pi/\omega_n$) and damping ratio ζ_n—of the nth mode of the MDF system, subjected to $\ddot{u}_g(t)$. It is governed by:

$$\ddot{D}_n + 2\zeta_n \omega_n \dot{D}_n + \omega_n^2 D_n = -\ddot{u}_g(t) \tag{12}$$

Substituting Eq. (11) into Eq. (9) gives the lateral displacements in the x and y directions and torsional rotations of the floors:

$$\mathbf{u}_{xn}(t) = \Gamma_n \boldsymbol{\phi}_{xn} D_n(t) \qquad \mathbf{u}_{yn}(t) = \Gamma_n \boldsymbol{\phi}_{yn} D_n(t) \qquad \mathbf{u}_{\theta n}(t) = \Gamma_n \boldsymbol{\phi}_{\theta n} D_n(t) \tag{13}$$

The story drifts in x and y directions defined at the CM are given by

$$\Delta_{jxn}(t) = \Gamma_n \left(\phi_{jxn} - \phi_{j-1,xn} \right) D_n(t) \qquad \Delta_{jyn}(t) = \Gamma_n \left(\phi_{jyn} - \phi_{j-1,yn} \right) D_n(t) \tag{14}$$

These equations can be generalized to define the story drifts for any frame, e.g., a frame at the edge of the building plan. Equations (13) and (14) represent the response of the MDF system to $\mathbf{p}_{\text{eff,n}}(t)$. Therefore, the response of the system due to total excitation $\mathbf{p}_{\text{eff}}(t)$ is

$$r(t) = \sum_{n=1}^{3N} r_n(t) \tag{15}$$

This is the UMRHA procedure for exact analysis of elastic systems, which is identical to the classical modal RHA. Equation (10) is the standard equation governing the modal coordinate $q_n(t)$, Eqs. (13) and (14) define the contribution of the nth mode to the response, and Eq. (15) combines the response contribution of all modes. However, these standard equations have been derived in an unconventional way. In contrast to the classical derivation found in textbooks (e.g., Ref. 23), we have used the modal expansion of the spatial distribution of the effective forces. This concept will provide a rational basis for the modal pushover analysis procedure to be developed later.

4.2   Inelastic Systems

Although modal analysis is not valid for an inelastic system, its response can be usefully discussed in terms of the modal coordinates of the corresponding elastic system. Each structural element of this elastic system is defined to have the same stiffness as the initial stiffness of the same structural element of the inelastic system. Both systems have the same mass and damping. Therefore, the natural vibration periods and modes of the corresponding elastic system are the same as the vibration properties—referred to as natural "periods" and "modes"—of the inelastic system undergoing small oscillation.

The response of an inelastic system to excitation $\mathbf{p}_{\text{eff,n}}(t)$ will no longer be described by Eq. (9) because "modes" other than the nth "mode" will also contribute to the response, implying that the vibration modes of the corresponding elastic system are now coupled; thus the floor displacements are given by the first part of Eq. (16):

$$\mathbf{u}_n(t) = \sum_{r=1}^{3N} \boldsymbol{\phi}_r q_r(t) \approx \boldsymbol{\phi}_n q_n(t) \tag{16}$$

However, because for linear systems $q_r(t) = 0$ for all modes other than the nth mode, it is reasonable to expect that $q_r(t)$ may be small and the nth "mode" should be dominant even for inelastic systems, implying that the elastic modes are, at most, weakly coupled.

This above-mentioned expectation is confirmed numerically in Fig. 6 for the original symmetric-plan building. Its response to excitation $\mathbf{p}_{\mathrm{eff,n}}(t)$ was determined by nonlinear RHA and the resulting roof displacement history was decomposed into its modal components. This building yields extensively when subjected to the selected ground motion and modes other than the nth "mode" contribute to the response. Other modes start responding as soon as the structure yields; however, their contributions to the roof displacement are generally very small, only a few percent, of the nth-"mode" contribution (Fig. 6a, c and e), implying weak coupling of elastic modes after the system yields. However, this is not always the case, as seen in the response to excitation $\mathbf{p}_{\mathrm{eff,2}}(t)$ in Fig. 6b. Although the contribution of the second mode is dominant, the first mode contribution is no longer very small, but is close to 25%.

The above-mentioned expectation is also confirmed numerically for unsymmetric-plan systems in Figs. 7 through 9, where the displacement of the frame at the right edge of the plan (Fig. 2) is plotted. The degree of modal coupling for the torsionally-stiff unsymmetric system U1 (Fig. 7) and for the torsionally-flexible unsymmetric system U3 (Fig. 9) is similar to that for the symmetric-building (Fig. 6). For system U1 modal coupling is seen to be insignificant for $\mathbf{p}_{\mathrm{eff,n}}(t)$ with n = 1, 2, and 4 (Fig. 7a, b, and d), but not for n = 3 (Fig. 7c), which denotes the mode similar to the second lateral vibration mode of the symmetric system. Although the contribution of the third mode is dominant, the first mode contribution is about 25%. For system U3, modal uncoupling is seen to be insignificant for $n = 1, 2,$ and 3 (Fig. 9a, b, and c), but not for n = 4 (Fig. 9d), which again denotes the mode similar to the second lateral vibration mode of the symmetric system. Although the contribution of the fourth mode is dominant, the second mode contribution is almost 25%. However, this modal coupling for n = 2 turns out to be stronger, as expected, for the unsymmetric system U2 (Fig. 8b), because it has very similar periods in pairs of torsionally-coupled modes; but, the modal coupling remains negligible for n = 1, 3, and 4 (Fig. 8a, c, and e).
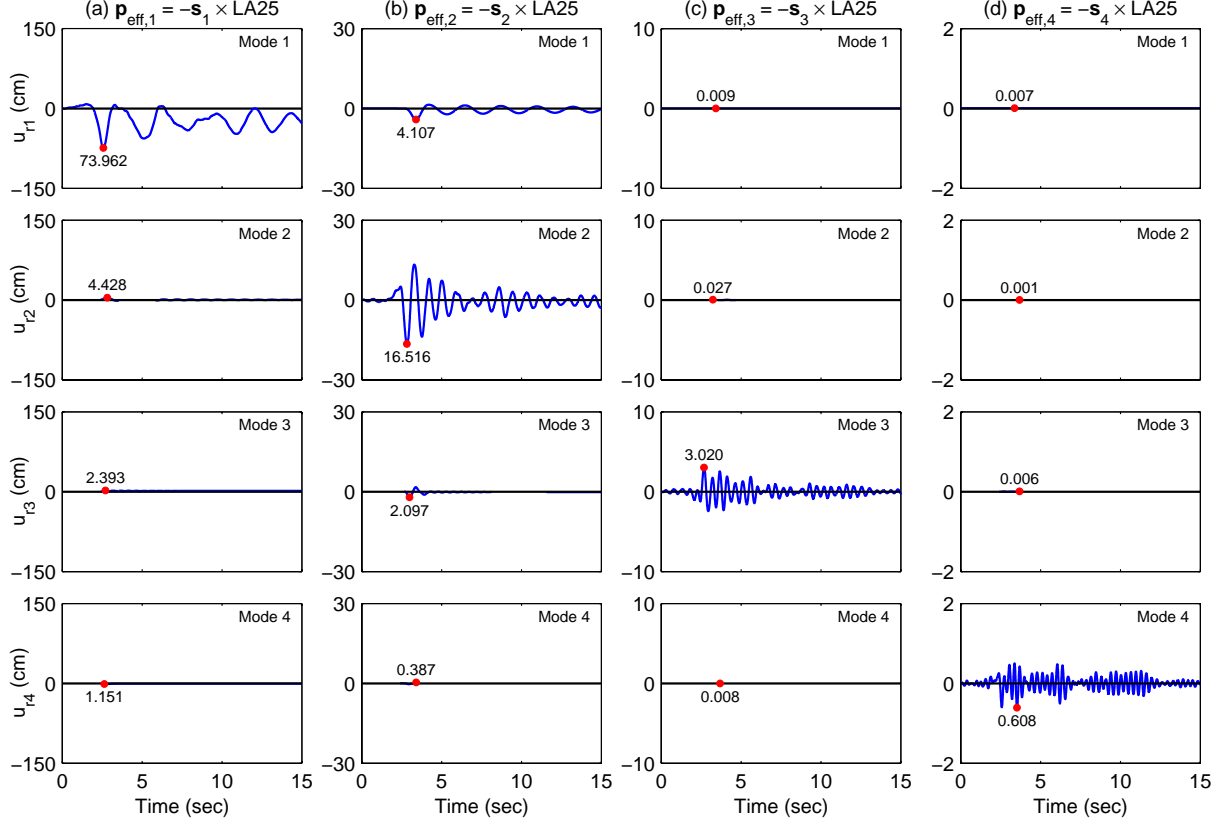
Figure 6. Modal decomposition of roof displacement at CM of the symmetric building: (a) $\mathbf{p}_{\text{eff},1} = -\mathbf{s}_1 \times \text{LA25}$; (b) $\mathbf{p}_{\text{eff},2} = -\mathbf{s}_2 \times \text{LA25}$; (c) $\mathbf{p}_{\text{eff},3} = -\mathbf{s}_3 \times \text{LA25}$; and (d) $\mathbf{p}_{\text{eff},4} = -\mathbf{s}_4 \times \text{LA25}$ **ground motion.**

These observations suggest that approximate analysis procedures based on the modal uncoupling approximation are expected to be as accurate for torsionally-stiff and torsionally-flexible buildings as they were for symmetric–plan buildings [15], but they may be less accurate for unsymmetric-plan buildings with very closely-spaced natural vibration periods. For many cases then, it is justified to approximate the structural response due to excitation $\mathbf{p}_{\text{eff,n}}(t)$ by the second half of Eq. (16) where $q_n(t)$ is governed by

$$\ddot{q}_n + 2\zeta_n \omega_n \dot{q}_n + \frac{F_{sn}}{M_n} = -\Gamma_n \ddot{u}_g(t) \tag{17}$$

and F_{sn} is a nonlinear hysteretic function of q_n:

$$F_{sn} = F_{sn}(q_n, \text{sign}\, \dot{q}_n) = \boldsymbol{\phi}_n^T \mathbf{f}_s(q_n, \text{sign}\, \dot{q}_n) \qquad (18)$$

If the smaller contributions of other modes had not been neglected, F_{sn} would depend on all modal coordinates, implying coupling of modal coordinates because of yielding of the structure.

With the above-stated approximation, the solution of Eq. (17) can be expressed as Eq. (11) where $D_n(t)$ is governed by

$$\ddot{D}_n + 2\zeta_n \omega_n \dot{q}_n + \frac{F_{sn}}{L_n} = -\ddot{u}_g(t) \qquad (19)$$

Figure 7. Modal decomposition of roof displacement at right frame of torsionally-stiff unsymmetric-plan system U1: **(a)** $\mathbf{p}_{\text{eff},1} = -\mathbf{s}_1 \times \text{LA25}$; **(b)** $\mathbf{p}_{\text{eff},2} = -\mathbf{s}_2 \times \text{LA25}$; **(c)** $\mathbf{p}_{\text{eff},3} = -\mathbf{s}_3 \times \text{LA25}$; and **(d)** $\mathbf{p}_{\text{eff},4} = -\mathbf{s}_4 \times \text{LA25}$ ground motion.
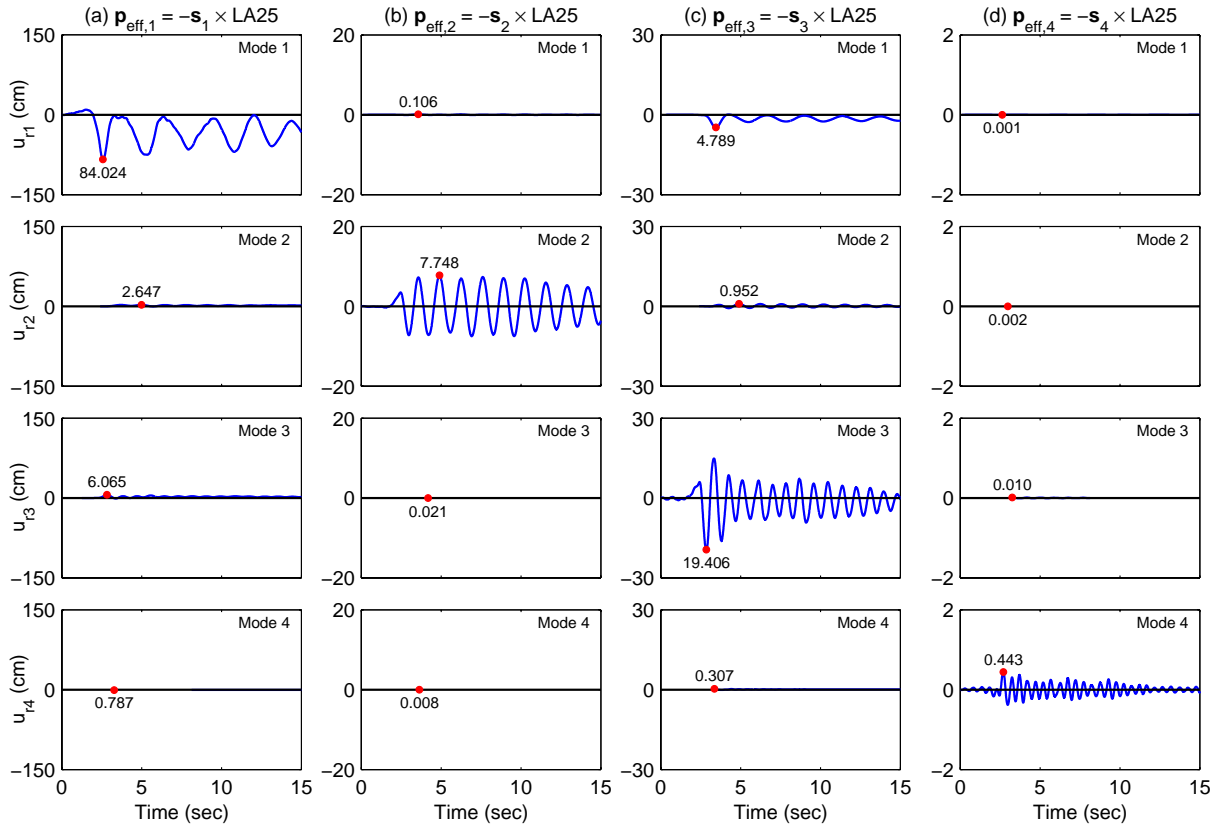
16

Figure 8. Modal decomposition of roof displacement at right frame of torsionally-similarly-stiff unsymmetric-plan system U2: (a) $\mathbf{p}_{\text{eff},1} = -\mathbf{s}_1 \times \text{LA25}$; (b) $\mathbf{p}_{\text{eff},2} = -\mathbf{s}_2 \times \text{LA25}$; (c) $\mathbf{p}_{\text{eff},3} = -\mathbf{s}_3 \times \text{LA25}$; and (d) $\mathbf{p}_{\text{eff},4} = -\mathbf{s}_4 \times \text{LA25}$ ground motion.
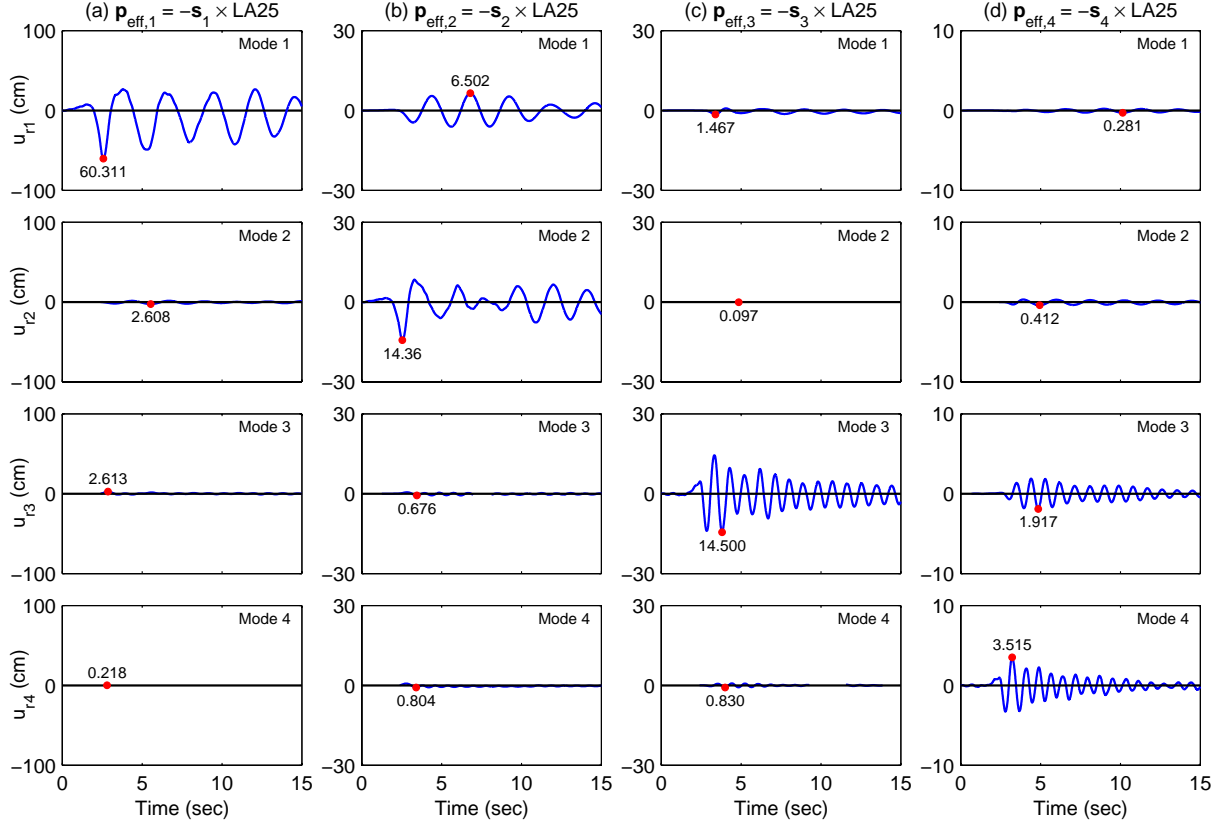
$D_n(t)$ may be interpreted as the deformation response of the nth-"mode" inelastic SDF system, an SDF system with (1) small-oscillation vibration properties—natural frequency and damping ratio ζ_n—of the nth mode of the corresponding linear system; and (2) $F_{sn}/L_n - D_n$ relation between resisting force and deformation, where

$$F_{sn} = F_{sn}\left(D_n, \text{sign } \dot{D}_n\right) = \boldsymbol{\phi}_n^T \mathbf{f}_s\left(D_n, \text{sign } \dot{D}_n\right) \tag{20}$$

which will be determined by nonlinear static or pushover analysis of the system using a modal force distribution based on Eq. (8). This procedure will be described later. Introducing the nth-mode inelastic SDF system permitted extension of the well-established concepts for elastic systems to inelastic systems; compare Eq. (10) to (17), Eq. (12) to (19), and note that Eq. (11) applies to both systems.
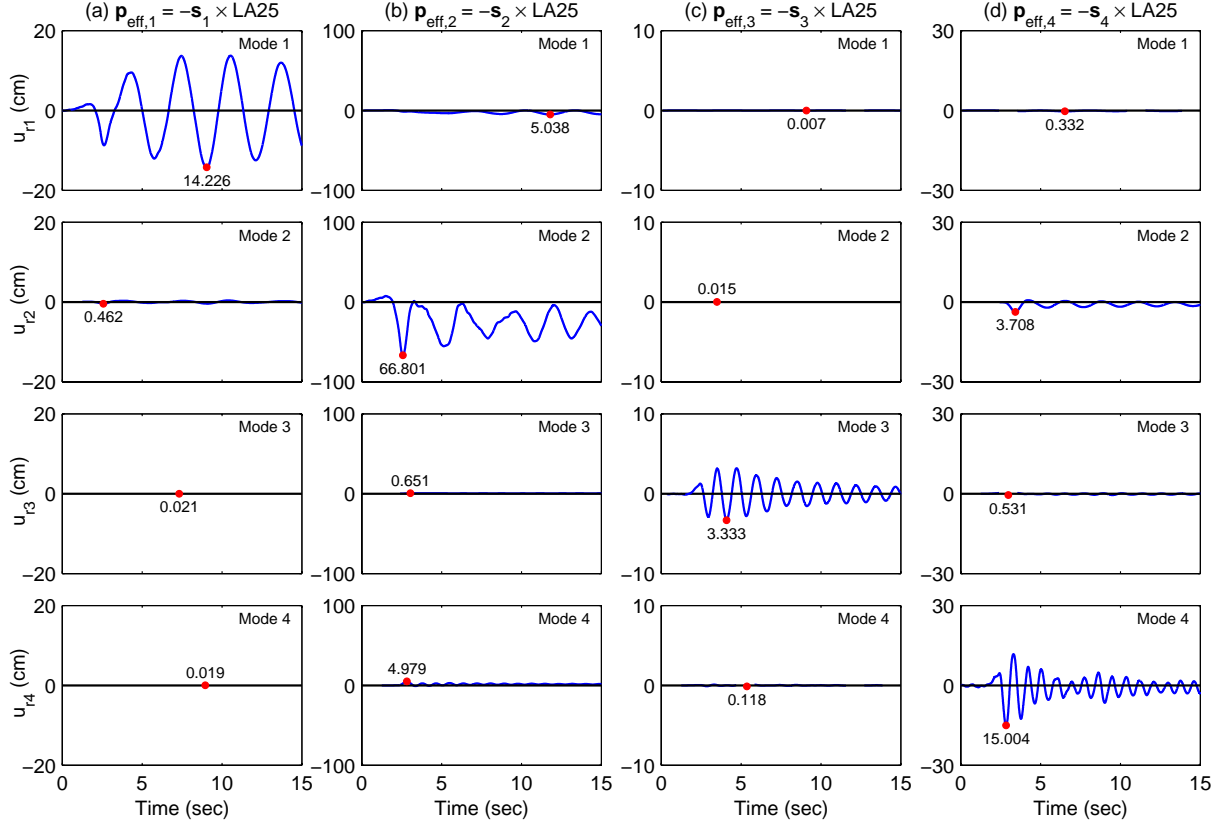
17

Figure 9. **Modal decomposition of roof displacement at right frame of torsionally-flexible system U3: (a)** $\mathbf{p}_{\text{eff},1} = -\mathbf{s}_1 \times \text{LA25}$**; (b)** $\mathbf{p}_{\text{eff},2} = -\mathbf{s}_2 \times \text{LA25}$**; (c)** $\mathbf{p}_{\text{eff},3} = -\mathbf{s}_3 \times \text{LA25}$**; and (d)** $\mathbf{p}_{\text{eff},4} = -\mathbf{s}_4 \times \text{LA25}$ **ground motion.**

Solution of the nonlinear Eq. (19) provides $D_n(t)$, which substituted into Eqs. (13) and (14) gives floor displacements and story drifts. Equations (13) and (14) approximate the response of the inelastic MDF system to $\mathbf{p}_{\text{eff,n}}(t)$, the nth-mode contribution to $\mathbf{p}_{\text{eff}}(t)$. The superposition of responses to $\mathbf{p}_{\text{eff,n}}(t)$, according to Eq. (15) to obtain the total response to $\mathbf{p}_{\text{eff}}(t)$, is strictly valid only for linearly elastic systems; however, it has been shown to be approximately valid for symmetric-plan inelastic systems [15]. This is the UMRHA procedure for approximate analysis of inelastic systems. When specialized for linearly elastic systems, it becomes identical to the rigorous classical modal RHA described earlier.

However, UMRHA is only an approximate analysis procedure for inelastic systems. To identify the underlying assumptions and approximations in UMRHA of inelastic systems, the

key equations in UMRHA for both classes of structural systems are compared. The striking similarity between the equations for the elastic and inelastic systems in apparent. Equations (11), (13), and (14) apply to both systems; Eqs. (10) and (12) differ from Eqs. (17) and (19) only in the resisting force; Eqs. (9) and (15) are exact for elastic systems but only approximate for inelastic systems. As is evident from Eq. (16), a principal approximation comes from neglecting the coupling of elastic modal coordinates [recall Eq. (18)] in computing the response of the inelastic system to $\mathbf{p}_{\text{eff,n}}(t)$. Supported by the numerical results of Figs. 7 through 9, this approximation is reasonable only because the excitation is the nth-mode contribution to the total excitation $\mathbf{p}_{\text{eff}}(t)$ [see Eq. (6)]. It would not be valid for an excitation with lateral force distribution different than $\mathbf{s}_n$, e.g., the total excitation $\mathbf{p}_{\text{eff}}(t)$.

To test this approximation, the response of three unsymmetric systems to $\mathbf{p}_{\text{eff,n}}(t) = -\mathbf{s}_n \ddot{u}_g(t)$, where $\ddot{u}_g(t)$ is the same ground motion as the one selected earlier, was determined by two methods and compared: (1) rigorous nonlinear RHA by solving the governing coupled equations [similar to Eq. (1) except that the right side is $\mathbf{p}_{\text{eff,n}}(t)$]; and (2) approximate UMRHA procedure. Such comparison for roof-displacement and top-story drift is presented in Figs. 10-12 and Figs. 13-15, respectively. The quality of the approximate results from UMRHA is seen to be uniformly good for the three systems: torsionally-stiff, torsionally flexible, and torsionally-similarly stiff. The errors in UMRHA results are slightly larger in drift than in displacement, but the errors in either response quantity seem acceptable for approximate methods to estimate seismic demands for unsymmetric-plan buildings.

The UMRHA procedure is based on Eq. (16), which restricts the deformations due to $\mathbf{p}_{\text{eff,n}}(t)$ to be proportional to the nth mode. This is exactly valid for linear elastic systems but is an approximation for inelastic systems. This approximation is avoided in the MPA procedure, which is presented next, but a modal combination approximation must be introduced as will be seen later. To provide a proper context, MPA is first presented for linear systems.

Figure 10. Comparison of approximate roof displacement of the right-frame of unsymmetric-plan system U1 from UMRHA and exact solution by nonlinear RHA for $\mathbf{p}_{\text{eff},n}(t) = -\mathbf{s}_n \ddot{u}_g(t)$, n = 1, 2, 3, and 4, where $\ddot{u}_g(t)$ = LA25 ground motion.

Figure 11. Comparison of approximate roof displacement of the right-frame of unsymmetric-plan system U2 from UMRHA and exact solution by nonlinear RHA for $\mathbf{p}_{\mathrm{eff},n}(t) = -\mathbf{s}_n \ddot{u}_g(t)$, n = 1, 2, 3, and 4, where $\ddot{u}_g(t)$ = LA25 ground motion.
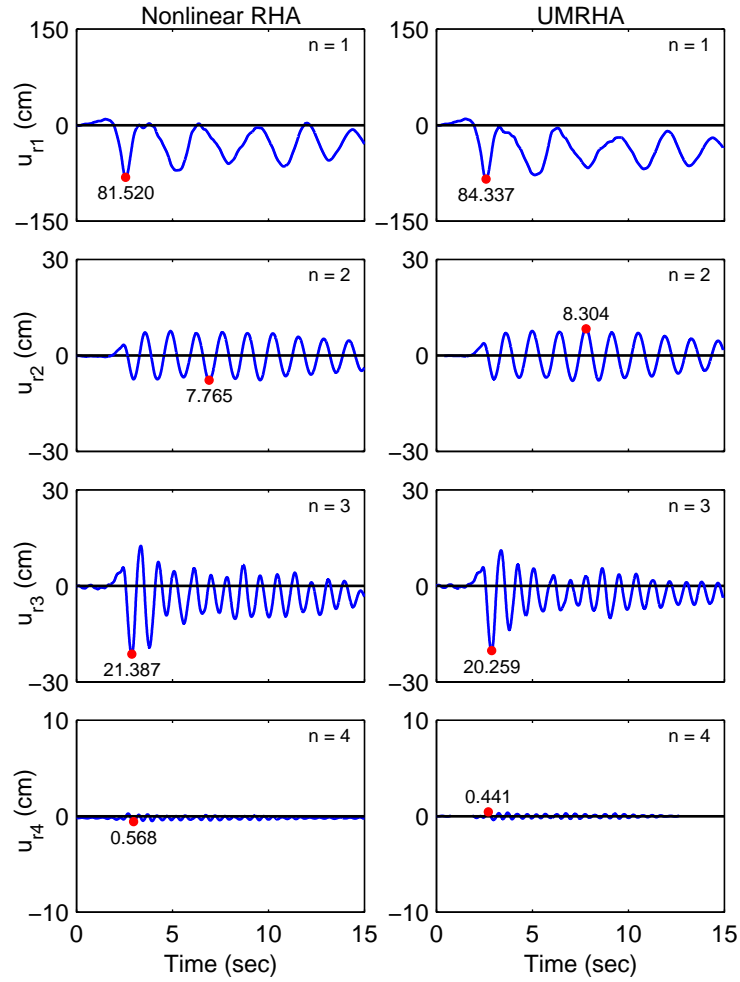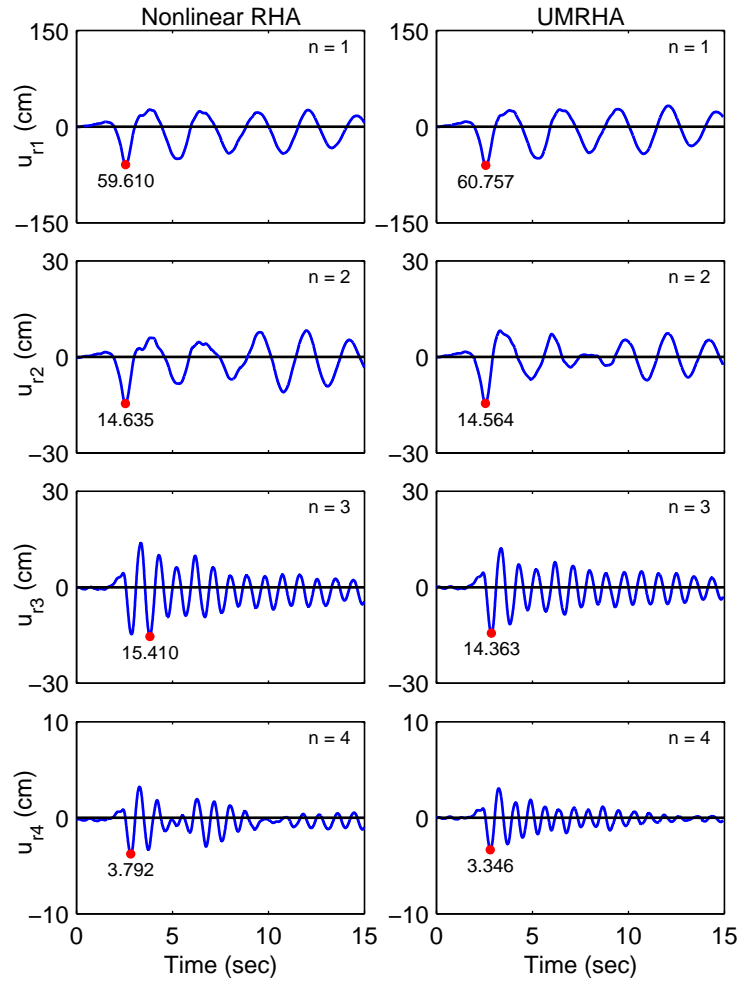
Figure 12. Comparison of approximate roof displacement of the right-frame of unsymmetric-plan system U3 from UMRHA and exact solution by nonlinear RHA for $\mathbf{p}_{\text{eff},n}(t) = -\mathbf{s}_n \ddot{u}_g(t)$ **,** *n* **= 1, 2, 3, and 4, where** $\ddot{u}_g(t)$ **= LA25 ground motion.**

Figure 13. Comparison of approximate top-story drift in right frame of unsymmetric-plan system U1 from UMRHA and exact solution by nonlinear RHA for $\mathbf{p}_{\mathrm{eff},n}(t) = -\mathbf{s}_n \ddot{u}_g(t)$, n = 1, 2, 3, and 4, where $\ddot{u}_g(t)$ = LA25 ground motion.

Figure 14. Comparison of approximate top-story drift in right frame of unsymmetric-plan system U2 from UMRHA and exact solution by nonlinear RHA for $\mathbf{p}_{\text{eff},n}(t) = -\mathbf{s}_n \ddot{u}_g(t)$ **,** *n* **= 1, 2, 3, and 4, where** $\ddot{u}_g(t)$ **= LA25 ground motion.**
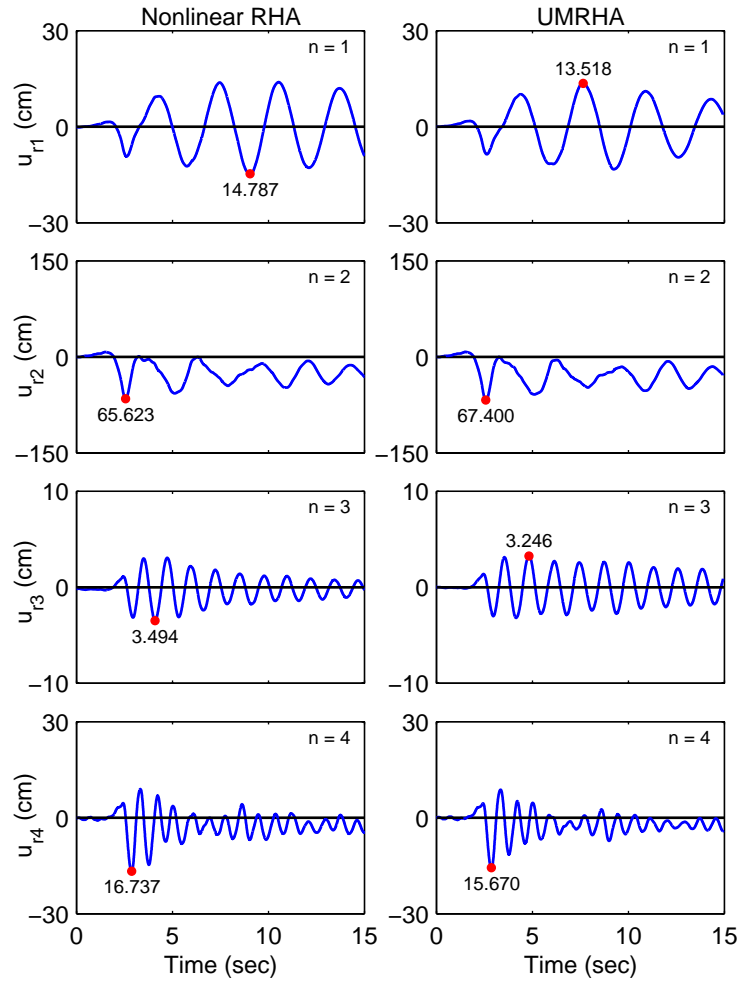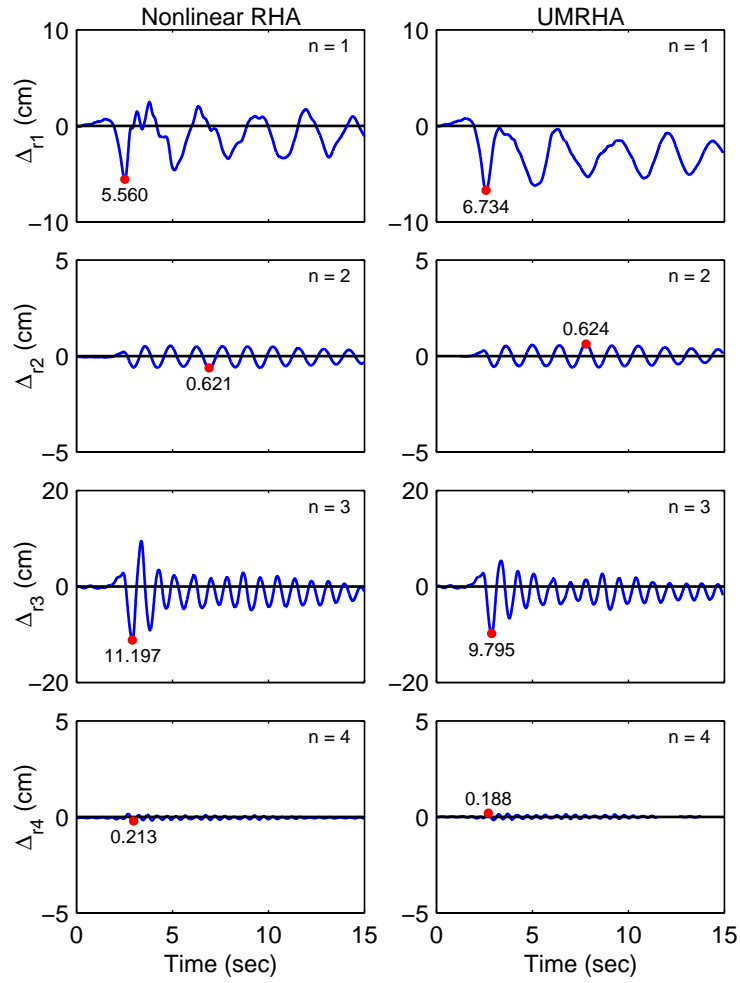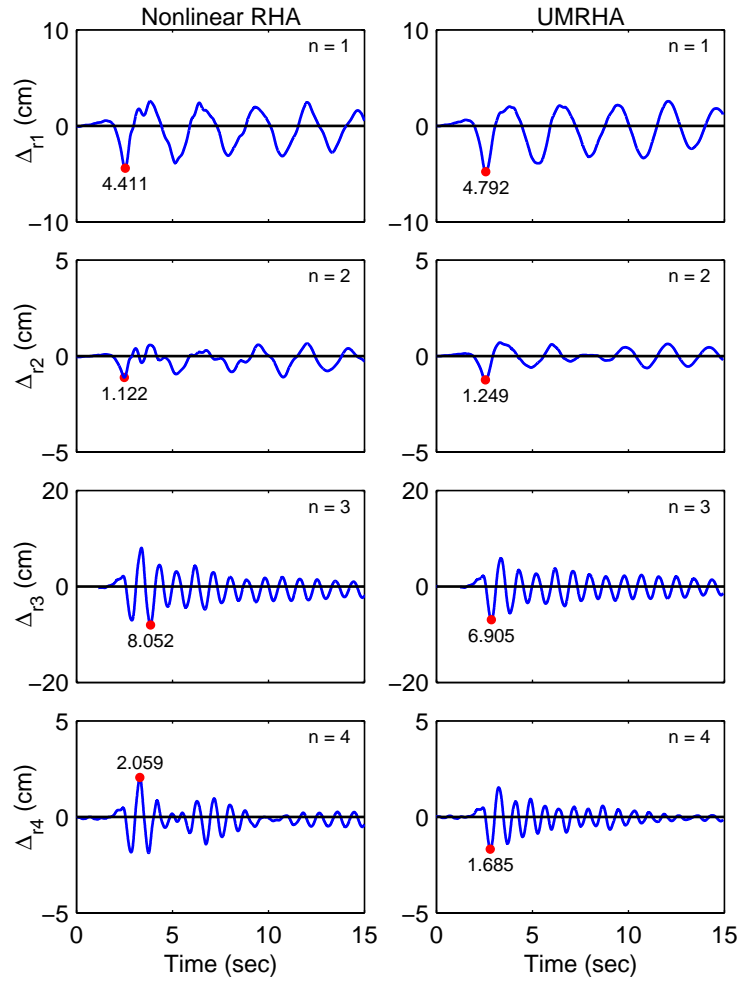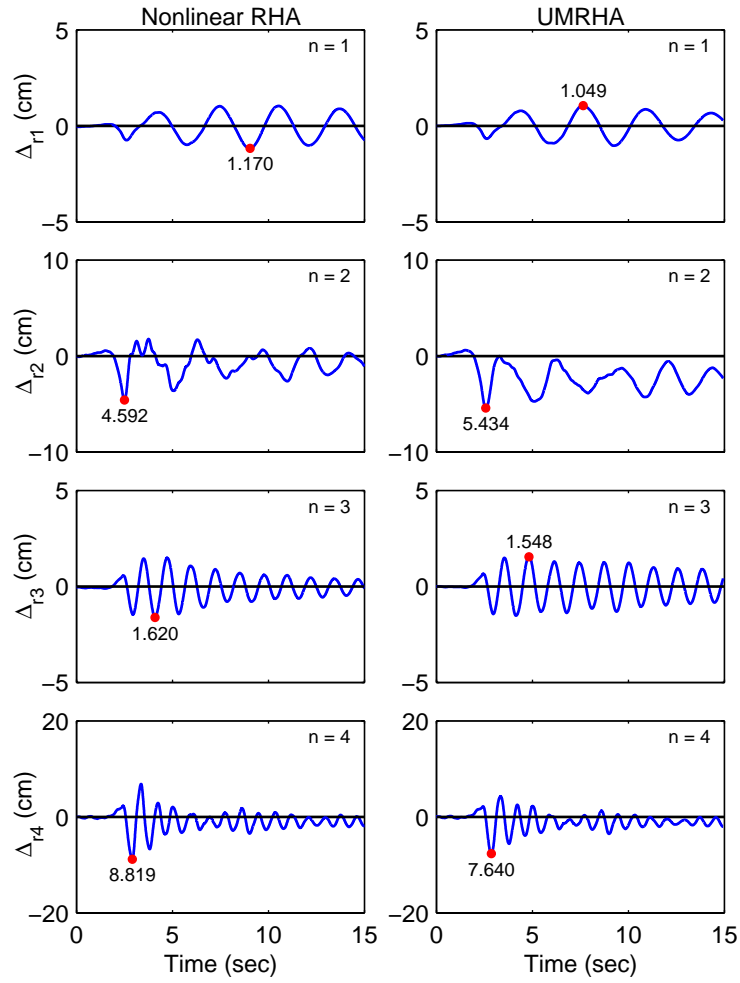
Figure 15. Comparison of approximate top-story drift in right frame of unsymmetric-plan system U3 from UMRHA and exact solution by nonlinear RHA for $\mathbf{p}_{\mathrm{eff},n}(t) = -\mathbf{s}_n \ddot{u}_g(t)$**,** *n* **= 1, 2, 3, and 4, where** $\ddot{u}_g(t)$ **= LA25 ground motion.**

5. MODAL PUSHOVER ANALYSIS

5.1 Elastic Systems

Consider the lateral forces $\mathbf{f}_{xn}$ and $\mathbf{f}_{yn}$ in x and y directions and torques $\mathbf{f}_{\theta n}$ defined as:

$$\mathbf{f}_{xn} = \mathbf{s}_{xn}A_n \qquad \mathbf{f}_{yn} = \mathbf{s}_{yn}A_n \qquad \mathbf{f}_{\theta n} = \mathbf{s}_{\theta n}A_n \tag{21}$$

where $\mathbf{s}_{xn}$, $\mathbf{s}_{yn}$, and $\mathbf{s}_{\theta n}$ are given by Eq. (8), $A_n = \omega_n^2 D_n$ and D_n is the peak deformation of the nth-mode linear SDF system, determined by solving Eq. (12) for $D_n(t)$. Note that A_n is also the ordinate $A(T_n, \zeta_n)$ of the earthquake pseudo-acceleration response (or design) spectrum for the nth-mode SDF system. Static analysis of the structure subjected to forces defined by Eq. (21) will provide the peak value r_n of the nth-mode contribution $r_n(t)$ to $r(t)$ [Ref. 23, Section 13.9]; recall that the $r_n(t)$ for floor displacements and story drifts is given by Eqs. (13) and (14).

Alternatively, this peak modal response can be obtained by static analysis of the structure subjected to lateral forces and torques defined by the modal force distribution $\mathbf{s}_n^*$:

$$\mathbf{s}_n^* = \begin{Bmatrix} \mathbf{m}\boldsymbol{\phi}_{xn} \\ \mathbf{m}\boldsymbol{\phi}_{yn} \\ \mathbf{I}_p\boldsymbol{\phi}_{\theta n} \end{Bmatrix} \tag{22}$$

with the structure pushed to the roof (or Nth floor) displacement:

$$u_{rxn} = \Gamma_n\phi_{rxn}D_n \qquad u_{ryn} = \Gamma_n\phi_{ryn}D_n \qquad u_{r\theta n} = \Gamma_n\phi_{r\theta n}D_n \tag{23}$$

where the subscript "r" denotes the roof . For elastic structures, $\mathbf{s}_n^*$ is the only force distribution that produces displacements proportional to the nth vibration mode. Therefore, the three components of roof displacement of an elastic system will simultaneously reach the values given by Eq. (23).

The peak modal response r_n, each determined by one modal pushover analysis, can be combined by the Complete Quadratic Combination (CQC) Rule [Ref. 23, Section 13.7], a rule suitable for unsymmetric-plan buildings, which may have closely-spaced frequencies of

vibration. This MPA procedure for linear elastic systems is identical to the standard response spectrum analysis (RSA) procedure.

5.2 Inelastic Systems

In the MPA procedure, the peak response r_n of the inelastic building to effective earthquake forces $\mathbf{p}_{\text{eff,n}}(t)$ is estimated by a nonlinear static analysis of the structure subjected to lateral forces and torques distributed over the building height according to $\mathbf{s}_n^*$ [Eq. (22)] with the forces increased to push the structure up to roof displacements u_{rxn}, u_{ryn}, $u_{r\theta n}$. These values of the roof displacement components are determined from Eq. (23), as for elastic systems, but D_n is now the peak deformation of the nth-"mode" inelastic SDF system, determined by solving Eq. (19) for $D_n(t)$. Alternatively, D_n can be determined from inelastic response (or design) spectrum [Ref. 23; Sections 7.6 and 7.12] or the elastic response (or design) spectrum in conjunction with empirical equations for inelastic deformation ratio [24]. At this roof displacement, nonlinear static analysis provides an estimate of the peak value r_n of response quantity $r_n(t)$: floor displacements, story drifts, and other deformation quantities.

For an inelastic system, no invariant distribution of forces will produce displacements proportional to the nth elastic mode. Therefore, the three components of roof displacement of an inelastic system will not simultaneously reach the values given by Eq. (23). One of the two lateral components will be selected as the controlling displacement; the choice of the component would be the same as the dominant motion in the mode being considered.

Nonlinear static analysis using force distribution $\mathbf{s}_n^*$ leads to the nth-"mode" pushover curve, a plot of base shear V_{bn} versus roof displacement u_{rn} in the appropriate (x or y) direction. Such pushover curves for the first four modes of the three unsymmetric-plan systems are shown in Figs. 16-18, wherein the roof displacements at the right and left frames are identified, indicating significant inelastic action in the right or the left frame for the more significant modes: first and third modes of system U1, all four modes of system U2, and second and fourth modes of system U3. The first-"mode" pushover curve and its bilinear idealization are shown in Fig. 19; at the yield point the base shear is V_{bn}^y and the roof displacement is u_{rn}^y.

Figure 16. "Modal" pushover curves of unsymmetric-plan system U1 with target displacements at the roof CM in the UMRHA and MPA analyses identified; also identified are the peak roof displacement at the right and left frames.

Figure 17. **"Modal" pushover curves of unsymmetric-plan system U2 with target displacements at the roof CM in the UMRHA and MPA analyses identified; also identified are the peak roof displacement at the right and left frames.**
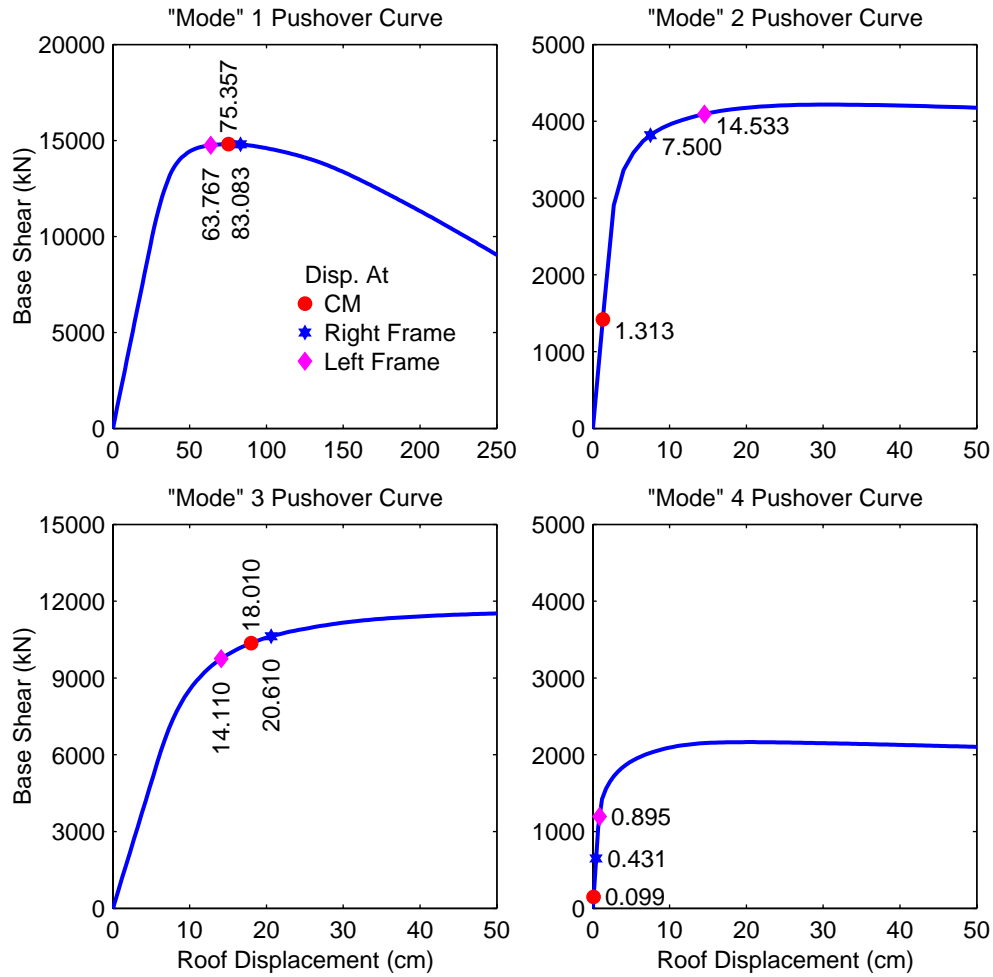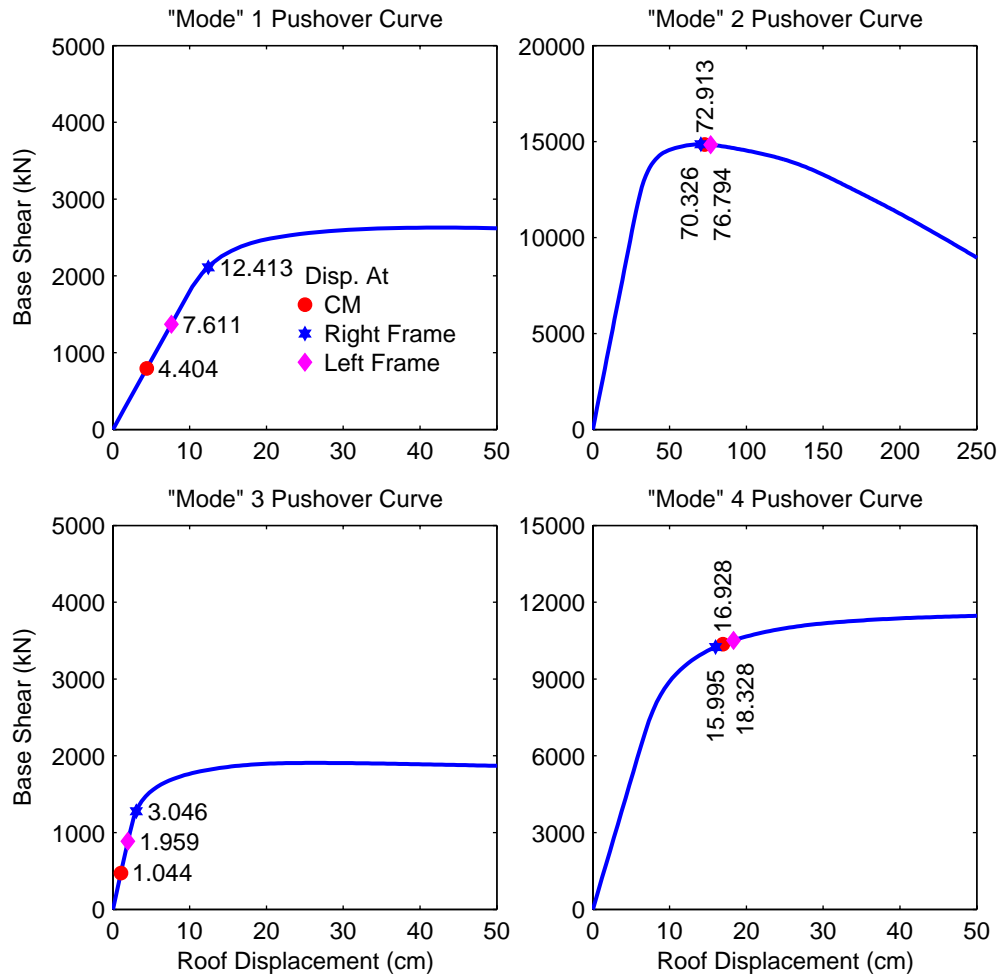
Figure 18. "Modal" pushover curves of unsymmetric-plan system U3 with target displacements at the roof CM in the UMRHA and MPA analyses identified; also identified are the peak roof displacement at the right and left frames.
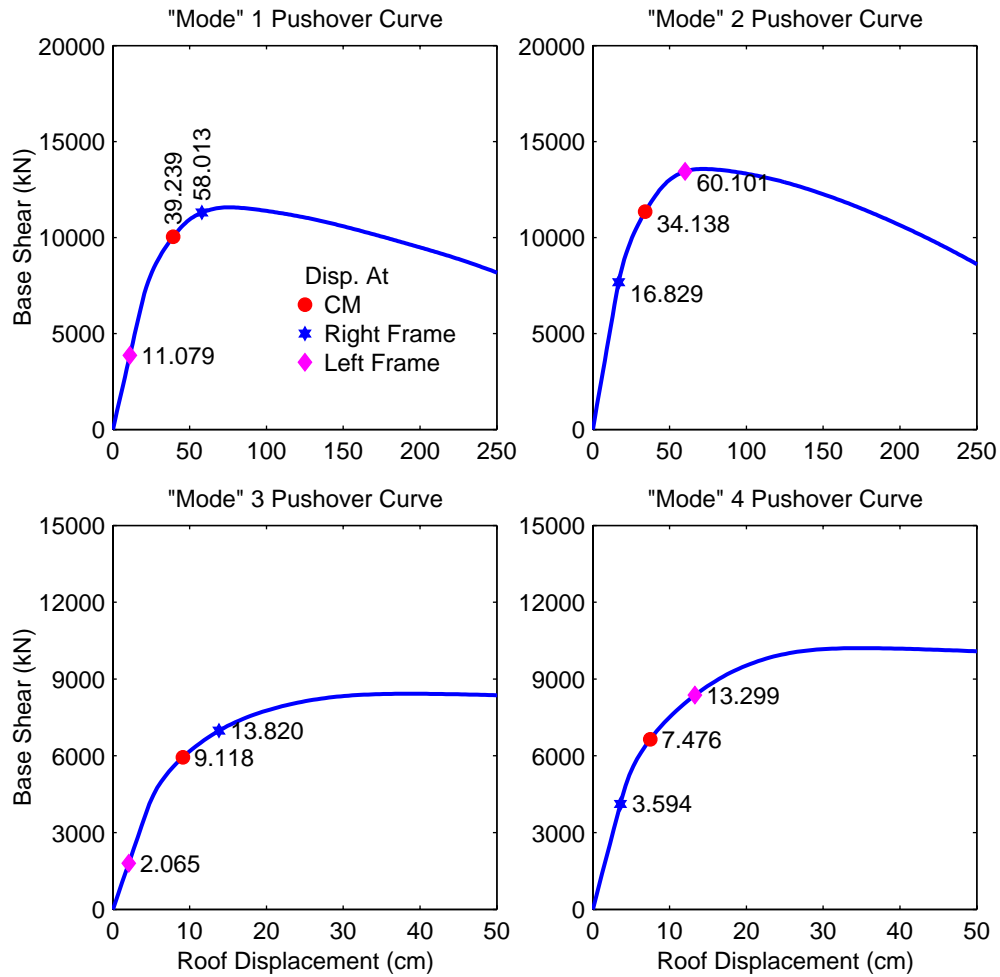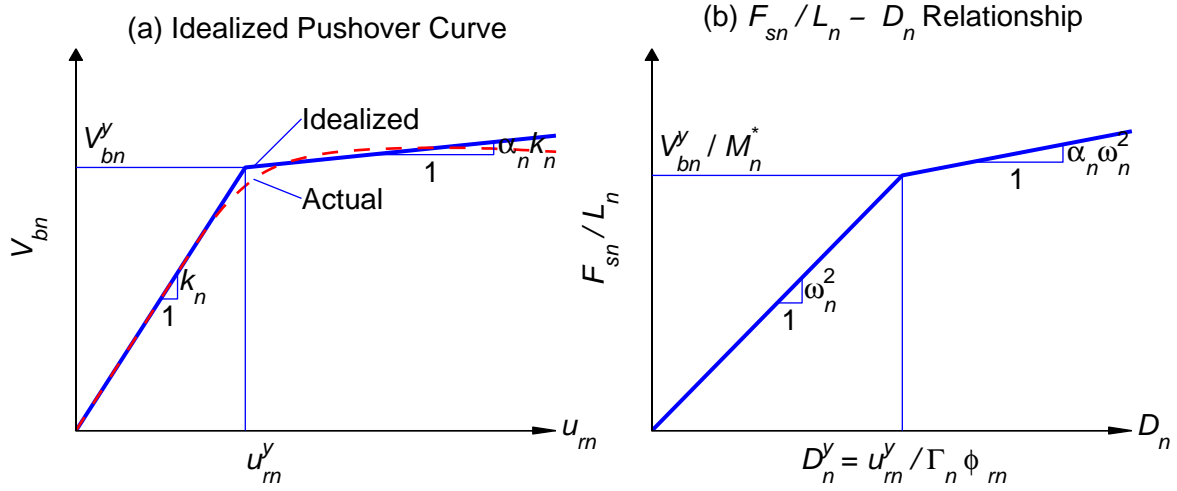
Figure 19. Properties of the *n*th-"mode" inelastic SDF system from the pushover curve.

The force deformation $\left(F_{sn}/L_n - D_n \right)$ relation for the *n*th-"mode" inelastic SDF system is required to determine D_n, whether it is determined by solving Eq. (19) for $D_n(t)$ or alternatively by response spectrum methods mentioned above. Based on the theory presented earlier [14] for symmetric-plan buildings, the $V_{bn} - u_{rn}$ pushover curve is converted to the desired $F_{sn}/L_n - D_n$ relation, as shown in Fig. 13b, where the yield values of F_{sn}/L_n and D_n are

$$\frac{F_{sn}^y}{L_n} = \frac{V_{bn}^y}{M_n^*} \qquad\qquad D_n^y = \frac{u_{rn}^y}{\Gamma_n \phi_{rn}} \tag{24}$$

in which $M_n^* = L_n \Gamma_n$ is the effective modal mass. The two are related through

$$\frac{F_{sn}^y}{L_n} = \omega_n^2 D_n^y \tag{25}$$

Knowing F_{sn}^y/L_n and D_n^y from Eq. (24), the elastic vibration period T_n of the *n*th-"mode" inelastic SDF system is computed from

$$T_n = 2\pi \left(\frac{L_n D_n^y}{F_{sn}^y} \right)^{1/2} \qquad (26)$$

In an unsymmetric-plan building the nonlinear static procedure leads to two pushover curves corresponding to the two lateral directions, x and y. In principle, both pushover curves will lead to the same $F_{sn}/L_n - D_n$ relation; thus, either one may be used. However, it would be natural to use the x (or y) pushover curve for a mode in which x (or y) component of displacements are dominant compared to their y (or x) component.

The response value r_n determined by pushover analysis is an estimate of the peak value of the response $r_n(t)$ of the inelastic structure to $\mathbf{p}_{\mathrm{eff,n}}(t)$; but it is not identical to another estimate determined by UMRHA. As mentioned earlier, r_n determined by pushover analysis of an elastic system is the exact peak value of $r_n(t)$, the nth-mode contribution to response $r(t)$. Thus we will refer to r_n as the peak "modal" response even in the case of inelastic systems. However, for inelastic systems the two estimates of the peak "modal" response are both approximate and different from each other; the only exception is the controlling component of the roof displacement. They differ because the underlying analyses involve different assumptions. UMRHA is based on the approximation contained in Eq. (16), which is avoided in MPA because the displacements, drifts, and other deformations are determined by nonlinear static analysis using force distribution $\mathbf{s}_n^*$. As a result, the floor displacements are no longer proportional to the mode shape, as implied by Eq. (16). In this sense, the MPA procedure represents the nonlinear behavior of the structure better than UMRHA.

However, the MPA procedure contains a different source of approximation, which does not exist in UMRHA. The peak "modal" response r_n, each determined by one pushover analysis, are combined by the CQC rule, just as for elastic systems. This application of modal combination rules to inelastic systems obviously lacks a rigorous theoretical basis, but seems reasonable because the modes are weakly coupled.

5.3 Summary of MPA

A step-by-step summary of the MPA procedure to estimate the seismic demands for an unsymmetric-plan multistory building is presented as a sequence of steps:

1. Compute the natural frequencies, ω_n and modes, $\boldsymbol{\phi}_n$, for linearly elastic vibration of the building.

2. For the nth-mode, develop the base shear-roof displacement, V_{bn}—u_{rn}, pushover curve by nonlinear static analysis of the building using the force distribution, $\mathbf{s}_n^*$ (Eq. 22). Between the two pushover curves obtained corresponding to two lateral directions, x and y, preferably choose the pushover curve in the dominant direction of motion of the mode. Gravity loads, including those present on the interior (gravity) frames, are applied before pushover analysis. Note the value of the lateral roof displacement due to gravity loads, u_{rg}.

3. Idealize the pushover curve as a bilinear curve. If the pushover curve exhibits negative post-yielding stiffness, the second stiffness (or post-yield stiffness) of the bilinear curve would be negative.

4. Convert the idealized V_{bn}—u_{rn} pushover curve to the force-displacement, F_{sn}/L_n—D_n, relation for the nth-"mode" inelastic SDF system by utilizing $F_{sn}^y/L_n = V_{bn}^y/M_n^*$ and $D_n^y = u_{rn}^y/\Gamma_n\phi_{rn}$ (Eq. 24) in which ϕ_{rn} is the value of $\boldsymbol{\phi}_n$ at the roof in the direction of the selected pushover curve; and M_n^* and Γ_n correspond to the direction of ground motion under consideration (x or y).

5. Compute the peak deformation D_n of the nth-"mode" inelastic single-degree-of-freedom (SDF) system defined by the force-deformation relation developed in Step 4 and damping ratio ζ_n. The elastic vibration period of the system is $T_n = 2\pi \left(L_n D_n^y / F_{sn}^y \right)^{1/2}$. For an SDF system with known T_n and ζ_n, D_n can be computed from nonlinear RHA, inelastic design spectrum, or elastic design spectrum in conjunction with empirical equations for the ratio of deformations of inelastic and elastic systems.

6. Calculate peak roof displacement u_{rn} in the direction of the selected pushover curve associated with the nth-"mode" inelastic SDF system from $u_{rn} = \Gamma_n \phi_{rn} D_n$.

7. From the pushover database (Step 2), extract values of desired responses r_{n+g} due to the combined effects of gravity and lateral loads at roof displacement equal to $u_{rn} + u_{rg}$.

8. Repeat Steps 3-7 for as many modes as required for sufficient accuracy.

9. Compute the dynamic response due to nth-"mode": $r_n = r_{n+g} - r_g$, where r_g is the contribution of gravity loads alone.

10. Determine the total response (demand) by combining gravity response and the peak "modal" responses using the CQC rule:

$$r \approx \max\left[r_g \pm \left(\sum_{i=1}^{J} \sum_{n=1}^{J} \rho_{in} r_i r_n \right)^{1/2} \right] \tag{27}$$

in which the correlation coefficient ρ_{in} is given by:

$$\rho_{in} = \frac{8\sqrt{\zeta_i \zeta_n} \left(\beta_{in} \zeta_i + \zeta_n \right) \beta_{in}^{3/2}}{\left(1 - \beta_{in}^2 \right)^2 + 4\zeta_i \zeta_n \beta_{in} \left(1 + \beta_{in}^2 \right) + 4\left(\zeta_i^2 + \zeta_n^2 \right) \beta_{in}^2} \tag{28}$$

where $\beta_{in} = \omega_i / \omega_n$ is the ratio of the ith and nth modal frequencies, and ζ_i and ζ_n are the damping ratios for these modes.

6.   EVALUTION OF THE MPA PROCEDURE

The MPA procedure was implemented for the original symmetric building and the three unsymmetric systems for the selected ground motion. To estimate the seismic demands, the contribution of the first three 'modes'' were included in analysis of the symmetric building and the first three "modal" pairs for the unsymmetric systems. The combined values of floor displacements and story drifts were computed including one, two, or three "modal" pairs (or modes for symmetric building). Figure 20a shows the floor displacements and story drift demands at the CM for the symmetric building together with the exact value determined by nonlinear RHA of the system. Figures 20b, c, and d show similar results for the three unsymmetric systems, but the demands are now for the frame at the right edge of the plan. These results lead to the following observations for unsymmetric systems, which also apply to symmetric buildings provided that all reference to "modal" pair(s) is replaced by mode(s).

As may be expected, the first "modal" pair alone is inadequate in estimating the story drifts, especially in the upper stories of the building (Fig. 20). Including the response contributions of higher "modal" pairs significantly improves the story drifts, but the floor displacements are unaffected, implying that contributions of the higher modal pairs to floor displacements are negligible. Two "modal" pairs suffice, implying that the contribution of the third "modal" pair is negligible.

Figure 20 shows that higher "modal" pairs contribute significantly to the seismic demands for the selected systems and MPA is able to capture these effects. With sufficient number of "modal" pairs included, the height-wise distribution of story drifts estimated by MPA is generally similar to the "exact" results from nonlinear RHA, and much superior to the first "modal" pair result. However, because MPA is an approximate method, it does not match the "exact" demands determining by nonlinear RHA. Instead MPA has the goal of estimating seismic demands to a useful degree of accuracy for practical application with the advantage of much less effort than required for nonlinear RHA.

For the excitation considered, the MPA results are accurate for two unsymmetric systems, U1 and U3, to a similar degree as they were for the symmetric building, which is apparent by comparing Figs. 20b and d with Fig. 20a; however, the results are less accurate for system U2. This loss of accuracy could be due to two reasons: The first plausible reason could be that the

system has very close modal periods and strong coupling of the lateral and torsional motions in each mode of vibration. However, in spite of the resulting stronger modal coupling (Fig. 8), the approximate UMRHA procedure was shown to be valid for this system (Fig. 11). Thus, strong lateral-torsional coupling does not seem to be the source of the entire discrepancy. Another plausible reason is that the roof displacement of system U2 due to the selected ground motion is considerably underestimated in the MPA procedure (Fig. 20c). This discrepancy occurs because the individual "modal" responses attain their peaks almost simultaneously (Fig. 11b), a situation for which the CQC modal combination rule is not valid. For such a case, the absolute sum (ABSSUM) rule (see Ref. 23, Section 13.7.2) may be more appropriate. To explore this possibility, Fig. 21 shows the floor displacements and story drifts determined by the MPA procedure using two different modal combination rules, CQC and ABSSUM, and compares these two estimates of seismic demand with its "exact" value determined by nonlinear RHA. The "exact" demand is generally bounded by the two estimates. The ABSSUM rule provides a conservative estimate of the roof displacement, as it should, and overestimates displacements at most floors and drifts in most stories. In contrast, for elastic systems, the ABSSUM rule would be conservative for all response quantities.

The preceding scenario points to the need for evaluating the MPA procedure considering an ensemble of ground motions and documenting the bias and dispersion in this procedure applied to unsymmetric buildings, as has been accomplished for symmetric buildings [15]. Such a statistical investigation is necessary for two reasons: First, the SRSS and CQC modal combination rules are based on random vibration theory and the combined peak response should be interpreted as the mean of the peak values of response to an ensemble of earthquake excitations. Thus, the modal combination rules are intended for use when the excitation is characterized by a smooth response (or design) spectrum. Although modal combination rules can also approximate the peak response to a single ground motion characterized by a jagged response spectrum, the errors are known to be much larger. Second, accurate estimation of roof displacement is necessary for the success of any pushover procedure and this usually is not possible for individual ground motions, as has been observed for the six SAC buildings [25]. For the Los Angeles 9-story building, the ratio of roof displacement values determined by MPA and nonlinear RHA varied from 0.66 to 1.70, with a median value of 1.21, over the 20 ground motions mentioned earlier.
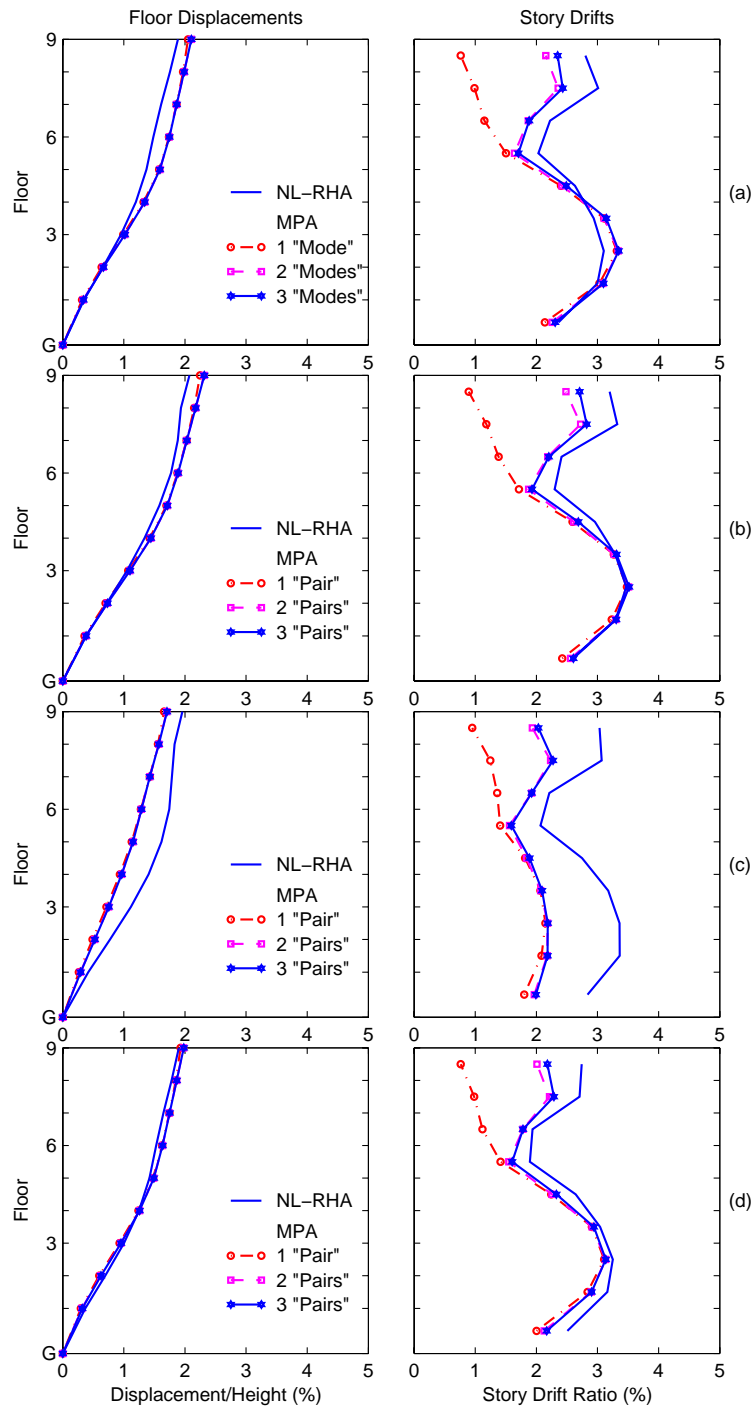
Figure 20. Floor displacements and story drifts determined by MPA with variable number of "modal" pairs (or modes) and nonlinear RHA: (a) symmetric building; (b) unsymmetric-plan system U1; (c) unsymmetric-plan system U2; and (d) unsymmetric-plan system U3.
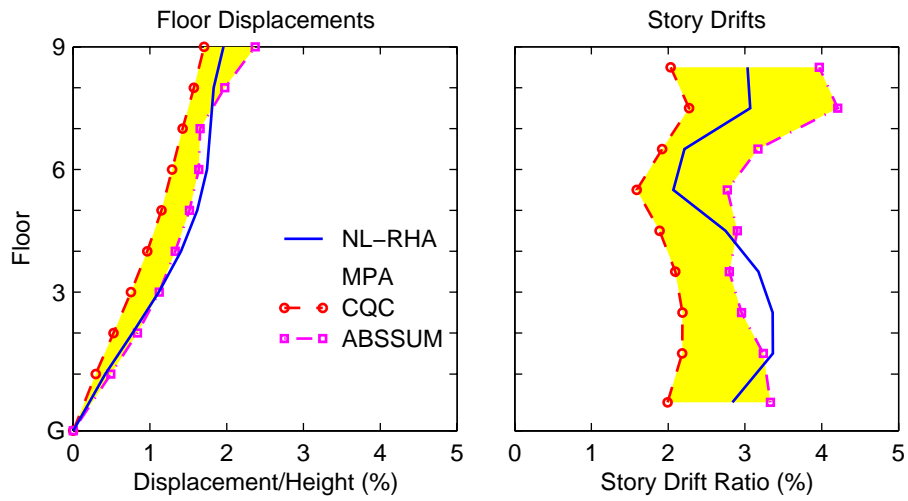
Figure 21. Floor displacements and story drifts at the right frame of unsymmetric-plan system U2 determined by MPA using CQC and ABSSUM combination rules and nonlinear RHA.

7. CONCLUSIONS

The Modal Pushover Analysis (MPA) procedure for estimating seismic demands has been extended to unsymmetric-plan buildings. Based on structural dynamics theory, the MPA procedure retains the conceptual simplicity of current procedures with invariant force distribution, now common in structural engineering practice.

The MPA estimate of seismic demand due to an intense ground motion (including a forward directivity pulse) has been shown to be generally accurate for unsymmetric systems to a similar degree as it was for a symmetric building. This conclusion is based on a comparison of the MPA estimate of demand and its exact value determined by nonlinear RHA for four structural systems: Los Angeles 9-story steel frame building designed for the SAC project and variations of this symmetric-plan building to create three unsymmetric-plan systems with different degrees of coupling between lateral and torsional motions, as characterized by different values of the ratio of uncoupled lateral and torsional vibration periods: torsionally-stiff system U1, torsionally-flexible system U3, and torsionally-similarly-stiff system U2. For the excitation considered, the MPA estimates for two unsymmetric systems, U1 and U3, are similarly accurate as they were for the symmetric-plan building; however, the results deteriorated for system U2 because of (a) stronger coupling of elastic modes and (b) underestimation of roof displacement by the CQC modal combination rule, which occurs because the individual modal responses attain their peaks almost simultaneously This implies that for system U2 and the selected ground motion the CQC modal combination rule would not give an accurate estimate of the peak response even if the system were linearly elastic.

This points to the need for evaluating the MPA procedure considering an ensemble of ground motions and documenting the bias and dispersion in the procedure applied to unsymmetric buildings, as has been accomplished for symmetric buildings [11]. Such future work will also evaluate the MPA procedure when earthquake hazard is defined by a design spectrum—typical of building codes and building evaluation guidelines—a situation for which modal combination rules were intended.

8. REFERENCES

[1] Building Seismic Safety Council (1997). NEHRP Guidelines for the Seismic Rehabilitation of Buildings, FEMA-273, Federal Emergency Management Agency, Washington, D.C.

[2] American Society of Civil Engineers (2000). Prestandard and Commentary for the Seismic Rehabilitation of Buildings, FEMA-356, Federal Emergency Management Agency, Washington, D.C.

[3] Fajfar, P., and Fischinger, M. (1988). N2—a method for nonlinear seismic analysis of regular structures, *Proc*., 9th World Conf. Earthq. Engrg., 5:111-116, Tokyo-Kyoto, Japan.

[4] Miranda, E. (1991). Seismic evaluation and upgrading if existing buildings, Ph.D. Dissertation, Dept. of Civil Engrg., University of California, Berkeley, Calif.

[5] Krawinkler, H., and Seneviratna, G. D. P. K. (1998). Pros and cons of a pushover analysis of seismic performance evaluation, *Engrg. Struc.,* 20(4-6):452-464.

[6] Naeim, F., and Lobo, R. M. (1998). Common pitfalls in pushover analysis, *Proc*., SEAOC Annual Convention, Reno, Nevada.

[7] Kim. B., and D'Amore, E. (1999). Pushover analysis procedure in earthquake engineering, *Earthq. Spectra*, 13(2):417-434.

[8] Elnashai, A. S. (2001). Advanced inelastic static (pushover) analysis for earthquake applications, *J. Struc. Engrg. Mech*., 12(1):51-69.

[9] Bracci, J. M., Kunnath, S. K., and Reinhorn, A. M. (1997). Seismic performance and retrofit evaluation for reinforced concrete structures, *J. Struc. Engrg*., ASCE, 123(1):3-10.

[10] Gupta, B., and Kunnath, S. K. (2000). Adaptive spectra-based pushover procedure for seismic evaluation of structures, *Earthq. Spectra*, 16(2):367-392.

[11] Sasaki, K. K., Freeman, S. A., and Paret, T. F. (1998). Multimode pushover procedure (MMP)—A method to identify the effects of higher modes in a pushover analysis, *Proc*., 6th U.S. Nat. Conf. Earthq. Engrg., Seattle, Washington.

[12] Kunnath, S. K., and Gupta, B. (2000). Validity of deformation demand estimates using nonlinear static procedures, *Proc*., U.S. Japan Workshop on Performance-Based Engineering for R/C Bldg. Struc., Sapporo, Hokkaido, Japan.

[13] Matsumori, T., Otani, S., Shiohara, H., and Kabeyasawa, T. (1999). Earthquake member deformation demands in reinforced concrete frame structures, *Proc*., U.S.-Japan Workshop on Performance-Based Earthq. Engrg. Methodology for R/C Bldg. Struc., pp. 79-94, Maui, Hawaii.

[14] Chopra, A. K., and Goel, R. K. (2002). A modal pushover analysis procedure for estimating seismic demands for buildings, *Earthq. Engrg. Struc. Dyn*., 31(3):561-582.

[15] Goel, R. K., and Chopra, A.K. (2004). Evaluation of Modal and FEMA pushover analyses: SAC buildings, *Earthq. Spectra*, to appear.

[16] Chintanapakdee, C, and Chopra, A. K. (2003). Evaluation of modal pushover analysis using generic frames, *Earthq. Engrg. Struc. Dyn*., 32(3):417-442.

[17] Chintanapakdee, C, and Chopra, A. K. (2004) Seismic response of vertically irregular frames: Response history and modal pushover analyses, ASCE, *J. Struc. Engrg.*, to appear.

[18] Kilar, V., and Fajfar, P. (1997). Simple push-over analysis of asymmetric buildings, *Earthq. Engrg. Struc. Dyn.*, 26(2):233-249.

[19] Moghadam, A. S., and Tso, W.-K. (1998). Pushover analysis for asymmetrical multistory buildings, *Proc.*, 6th U.S. Nat. Conf. Earthq. Engrg., EERI, Oakland, Calif., 13 pgs.

[20] De Stefano, M., and Rutenberg, A. (1998). Predicting the dynamic response of asymmetric multistory wall-frame structures by pushover analysis: two case studies, *Proc.*, 11th Eur. Conf. Earthq. Engrg., A.A. Balkema, Rotterdam.

[21] Faella, G., and Kilar, V. (1998). Asymmetric multistory R/C frame structures: push-over versus nonlinear dynamic analysis, *Proc.,* 11th Eur. Conf. Earthq. Engrg., A.A. Balkema, Rotterdam.

[22] Gupta, A. and Krawinkler, H. (1999). Seismic demands for performance evaluation of steel moment resisting frame structures (SAC Task 5.4.3), *Report No. 132*, John A. Blume Earthq. Engrg. Center, Stanford Univ., Stanford, Calif.

[23] Chopra, A.K. (2001). *Dynamics of Structures: Theory and Applications to Earthquake Engineering*. 2nd Edition, New Jersey: Prentice Hall.

[24] Chopra, A. K., and Chintanapakdee, C., (2003). Inelastic deformation ratios for design and evaluation of structures: Single-degree-of-freedom bilinear systems, ASCE, *J. Struc. Engrg.*, to appear.

[25] Chopra, A. K., Goel, R. K., and Chintanapakdee, C. (2003). Statistics of single-degree-of-freedom estimate of displacements for pushover analysis of buildings, ASCE, *J. Struc. Engrg.*, 129:1-11.

APPENDIX A: LOS ANGELES 9-STORY SAC BUILDING

The 9-story structure, shown in Fig. A-1, was designed by Brandow & Johnston Associates[*] for the SAC[**] Phase II Steel Project. Although not actually constructed, this structure meets seismic code requirements of the 1994 UBC and represents typical medium-rise buildings designed for the Los Angeles, California, region.

A benchmark structure for the SAC project, this building is 45.73 m (150 ft) by 45.73 m (150 ft) in plan, and 37.19 m (122 ft) in elevation. The bays are 9.15 m (30 ft) on center, in both directions, with five bays each in the north-south (N-S) and east-west (E-W) directions. The building's lateral force-resisting system is composed of steel perimeter moment-resisting frames (MRFS). To avoid bi-axial bending in corner columns, the exterior bay of the MRF has only one moment-resisting connection. The interior bays of the structure contain frames with simple (shear) connections. The columns are 345 MPa (50 ksi) steel wide-flange sections. The levels of the 9-story building are numbered with respect to the ground level (see Fig. A.1) with the ninth level being the roof. The building has a basement level, denoted B-1. Typical floor-to-floor heights (for analysis purposes measured from center-of-beam to center-of-beam) are 3.96 m (13 ft). The floor-to-floor height of the basement level is 3.65 m (12 ft) and for the first floor is 5.49 m (18 ft).

The column lines employ two-tier construction, i.e., monolithic column pieces are connected every two levels beginning with the first level. Column splices, which are seismic (tension) splices to carry bending and uplift forces, are located on the first, third, fifth, and seventh levels at 1.83 m (6 ft) above the center-line of the beam to column joint. The column bases are modeled as pinned and secured to the ground (at the B-1 level). Concrete foundation walls and surrounding soil are assumed to restrain the structure at the ground level from horizontal displacement.

The floor system is composed of 248 MPa (36 ksi) steel wide-flange beams in acting composite action with the floor slab. The seismic mass of the structure is due to various components of the structure, including the steel framing, floor slabs, ceiling/flooring,

---

[*] Brandow & Johnston Associates, Consulting Structural Engineers, 1660 W. Third St., Los Angeles, CA 90017.
[**] SAC is a joint venture of three non-profit organizations: The Structural Engineers Association of California (SEAOC), the Applied Technology Council (ATC), and California Universities for Research in Earthquake Engineering (CUREE). SAC Steel Project Technical Office, 1301 S. 46th Street, Richmond, CA 94804-4698.

mechanical/electrical, partitions, roofing and a penthouse located on the roof. The seismic mass of the ground level is 9.65×10^5 kg (66.0 kips-sec^2/ft), for the first level is 1.01×10^6 kg (69.0 kips-sec^2/ft), for the second through eighth levels is 9.89×10^5 kg (67.7 kips-sec^2/ft), and for the ninth level is 1.07×10^6 kg (73.2 kips-sec^2/ft). The seismic mass of the above ground levels of the entire structure is 9.00×10^6 kg (616 kips- sec^2/ft).

The three-dimensional building model, implemented in OpenSees[+], consists of four perimeter MRFs (Fig. 2), two in each direction, connected by rigid floor diaphragms at each floor level; Fig. A1 shows details of a typical frame. Such a three-dimensional model has three DOFs per floor: two translational in the x- and y-directions, and one rotational about the vertical axis. The translational and rotational degrees-of-freedom at CM of the ground floor level are restrained to represent effects of stiff basement walls.

The model is assigned translational masses in the x- and y-directions equal to m_j and a rotational mass (or moment of inertia) equal to I_{Oj} about a vertical axis at CM of the each floor level; I_{Oj} is computed by assuming that the mass m_j is uniformly distributed over the floor plan. The model is based on centerline dimensions of the bare frames in which beams and columns extend from centerline to centerline. The beams and columns are modeled with nonlinear beam-column elements in OpenSees with fiber sections; this element considers spread of plasticity across the section depth and the element length. The effects of gravity loads on interior gravity-load carrying frames are modeled by including a P-Δ column at the geometric center of the model. The strength, dimension, and shear distortion of panel zones are neglected but large deformation (P–Δ) effects are included.

[+] Mazzoni, S., McKenna, F., Scott, M.H., Fenves, G.L., and Jeremic, B. (2003). Open System for Earthquake Engineering Simulation (OpenSees): Command Language Manual, Pacific Earthquake Engineering Center, University of California, Berkeley, http://opensees.berkeley.edu.
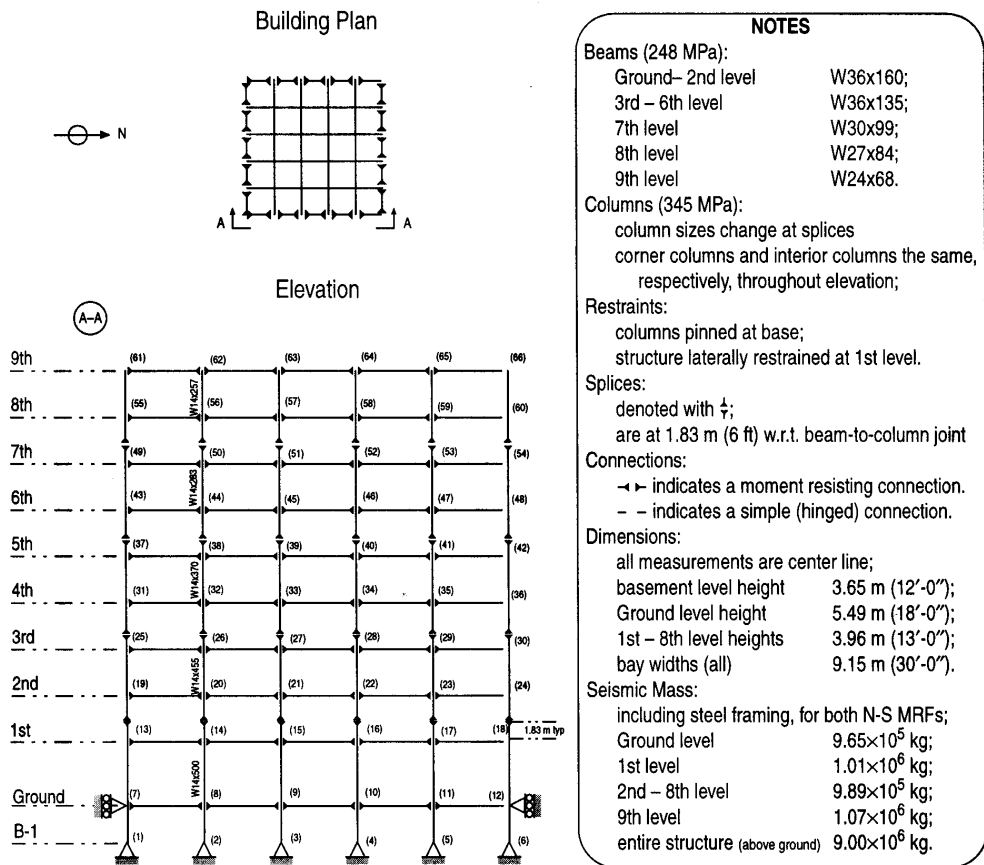
Building Plan

Elevation

NOTES

Beams (248 MPa):
- Ground– 2nd level   W36x160;
- 3rd – 6th level   W36x135;
- 7th level   W30x99;
- 8th level   W27x84;
- 9th level   W24x68.

Columns (345 MPa):
- column sizes change at splices
- corner columns and interior columns the same, respectively, throughout elevation;

Restraints:
- columns pinned at base;
- structure laterally restrained at 1st level.

Splices:
- denoted with $\frac{1}{T}$;
- are at 1.83 m (6 ft) w.r.t. beam-to-column joint

Connections:
- ◄► indicates a moment resisting connection.
- – – indicates a simple (hinged) connection.

Dimensions:
- all measurements are center line;
- basement level height   3.65 m (12′-0″);
- Ground level height   5.49 m (18′-0″);
- 1st – 8th level heights   3.96 m (13′-0″);
- bay widths (all)   9.15 m (30′-0″).

Seismic Mass:
- including steel framing, for both N-S MRFs;
- Ground level 9.65×10^5 kg;
- 1st level 1.01×10^6 kg;
- 2nd – 8th level 9.89×10^5 kg;
- 9th level 1.07×10^6 kg;
- entire structure (above ground) 9.00×10^6 kg.

Fig. A-1. Nine-story building [adapted from Ohtori, Y., Christenson, R. E., Spencer, B. F., Jr., and Dyke, S. J. (2000). Benchmark Control Problems for Seismically Excited Nonlinear Buildings, http://www.nd.edu/~quake/, Notre Dame University, Indiana.]

45